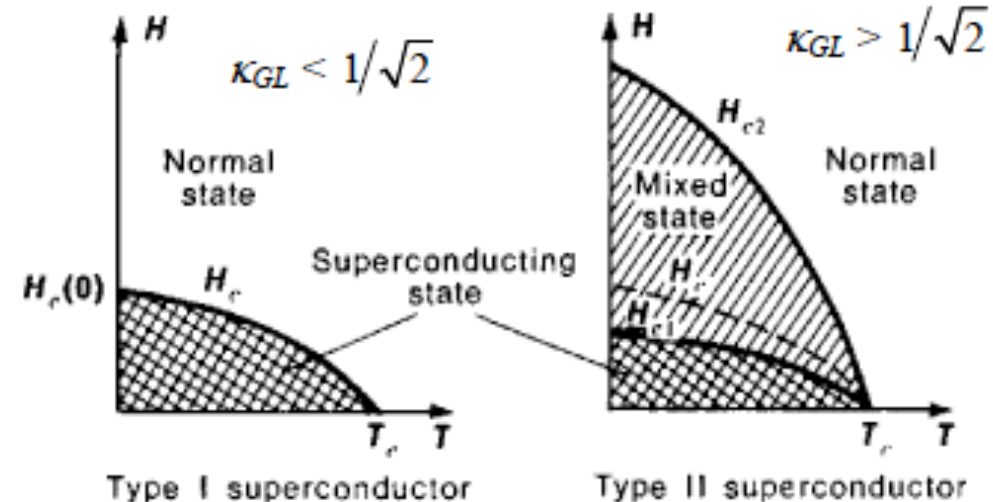
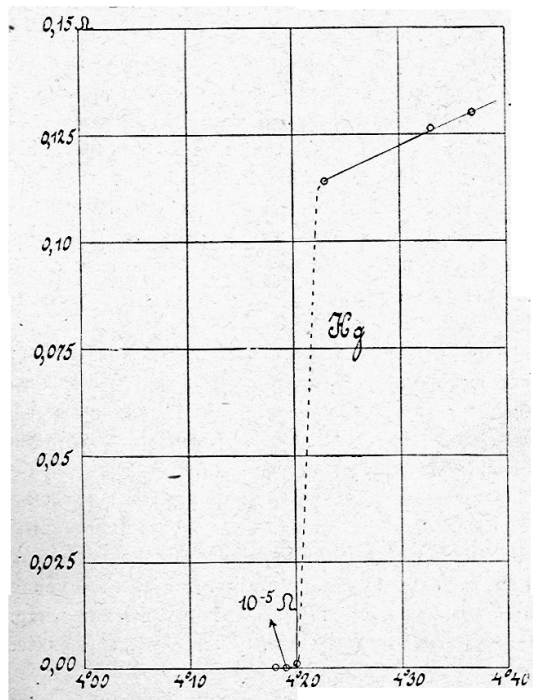


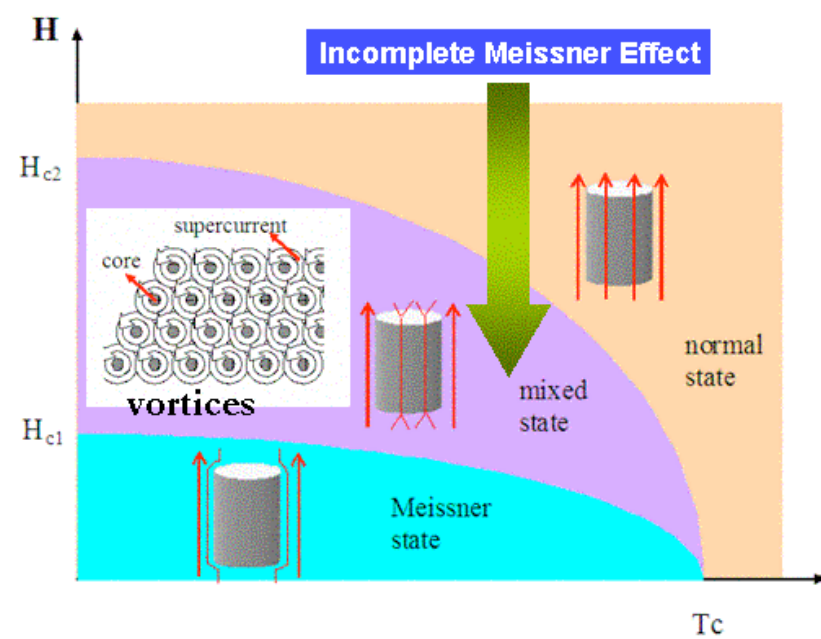
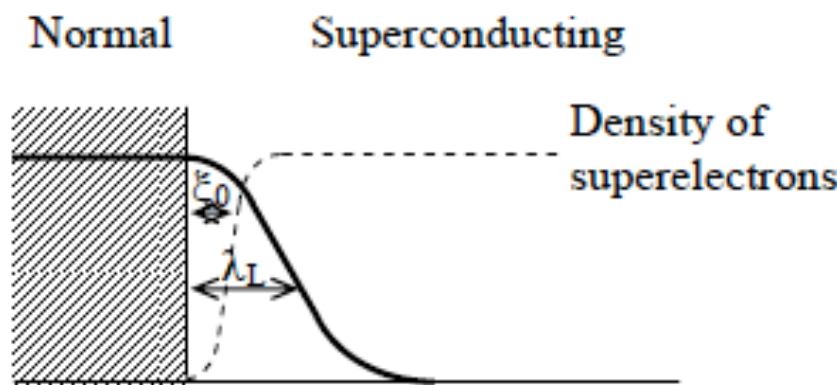
Muon Spin Rotation/Relaxation Studies of Niobium for SRF Applications

Anna Grassellino, Ph.D. Candidate, University of Pennsylvania

Superconductivity

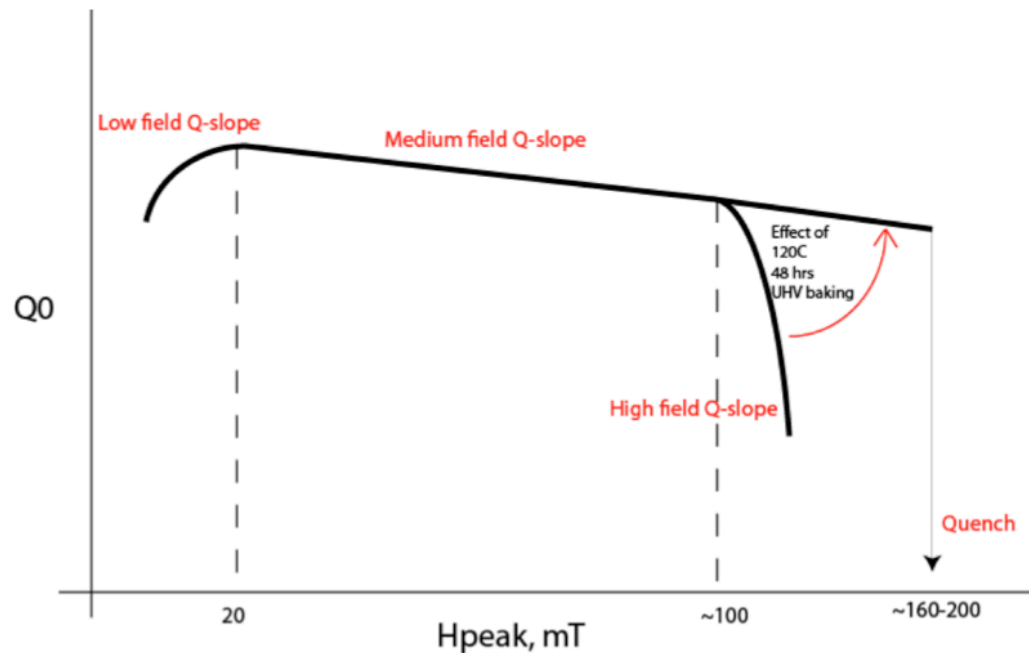


Nb: (marginal) type 2



Q-slope in Nb cavities

- Degradation of quality factor with the applied RF field
- Medium field Q-slope: gradual decrease in range $H_{pk} \sim 20-100$ mT
- **Problem we want to study: High field Q-drop: sharp losses above peak field $\sim 80-100$ mT**
- HFQS signature: 120C bake 48 hrs UHV improves/removes HFQS



- Huge number of models in the history of SRF to explain HFQS
- **None so far unconfutably proves causes or mechanisms**

HFQS: early magnetic flux entry?

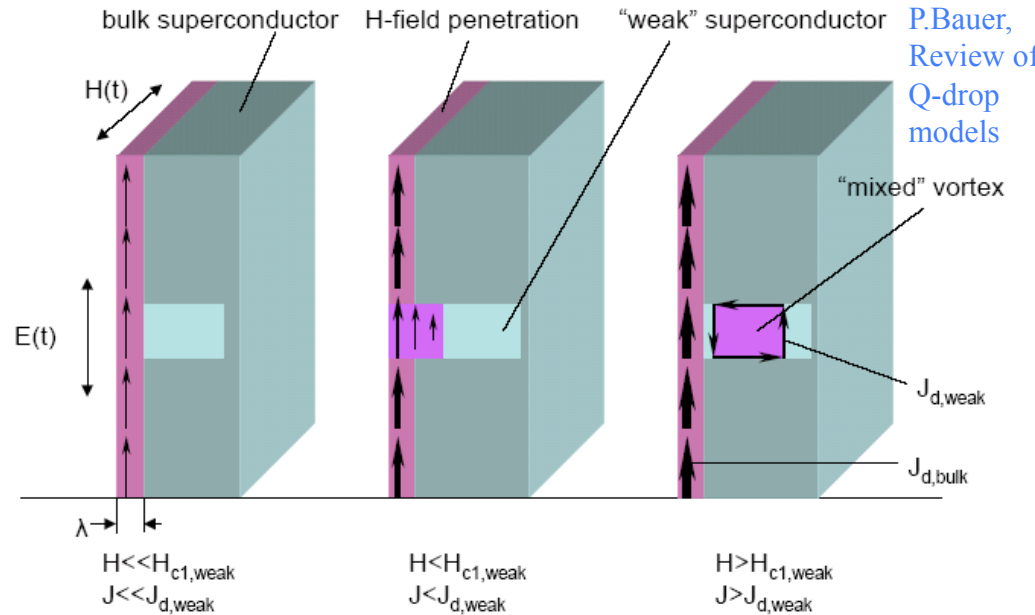


Table 1. H_p and H_{c2} at 2 K and T_c of various samples of Nb.

Sample	T_c (K)	H_p (Oe)	H_{c2} (Oe)
Nb S ₁ -LG	9.2	1800	6500
Nb S ₂ -LG	9.05	1050	3700
Nb S ₃ -LG	9.08	1250	3800
Nb S ₁ -FG	9.26	1600	7500
Nb S ₂ -FG	9.05	950	3800
Nb S ₃ -FG	9.08	1100	4000

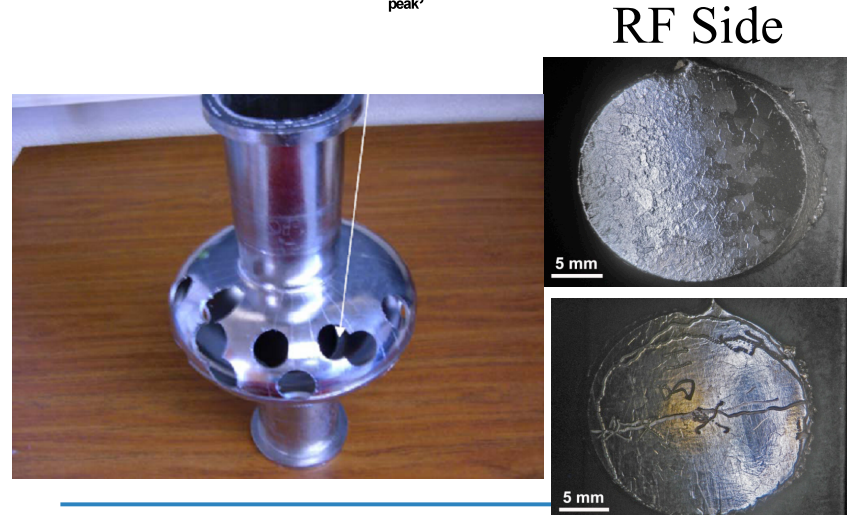
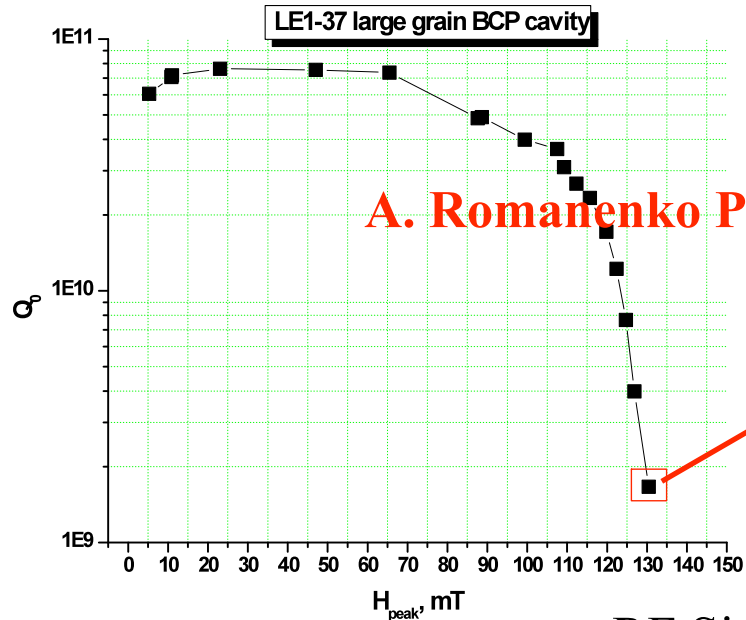
Roy et al, Supercond. Sci. Technol. 22 (2009) 105014

- ‘Weaker’ superconducting regions allow ‘premature’ magnetic flux entry in the Nb surface
- Model never proved, but there are experimental hints towards it, eg:
 - Magnetization measurements of Nb samples with different treatments (Roy, Myneni): field of entry varies in agreement with RF cavity performance
 - Cutout samples studies (Romanenko, Padamsee): decrease in average dislocation density observed by EBSD after 120C baking -working hypothesis – surface dislocations provide sites for early flux penetration (below bulk H_{c1})

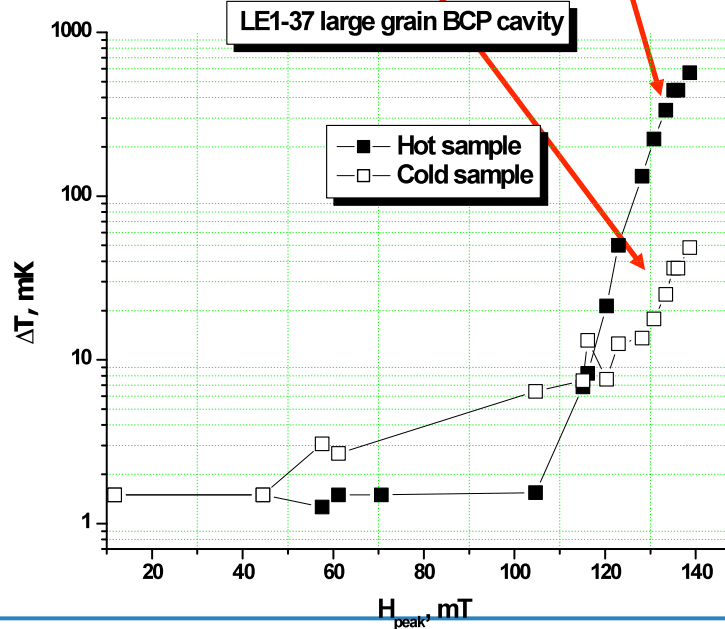
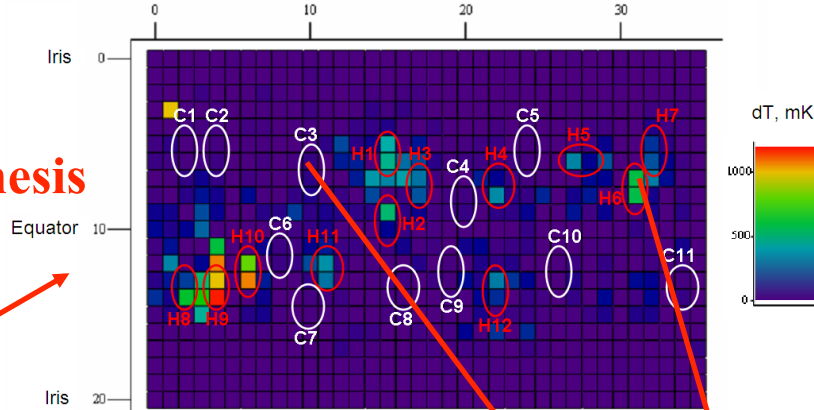
HFQS: how to prove if it's early flux penetration?

- **GOAL:** Design an experiment to prove magnetic flux entry as the right or wrong mechanism behind HFQS
- We study for the first time the field of first flux entry in RF characterized samples → HFQS limited cutout samples:
 - Hot vs cold
 - **Baked vs unbaked**
- Look for correlation field of flux entry – onset of HFQS (as per thermometry characterization and after surface treatments like 120C baking and BCP)
- Need of local, sensitive magnetic field probe: **Muon Spin Rotation**
- We will see that the probe is able to measure with extreme precision what fraction of the sample contains magnetic flux

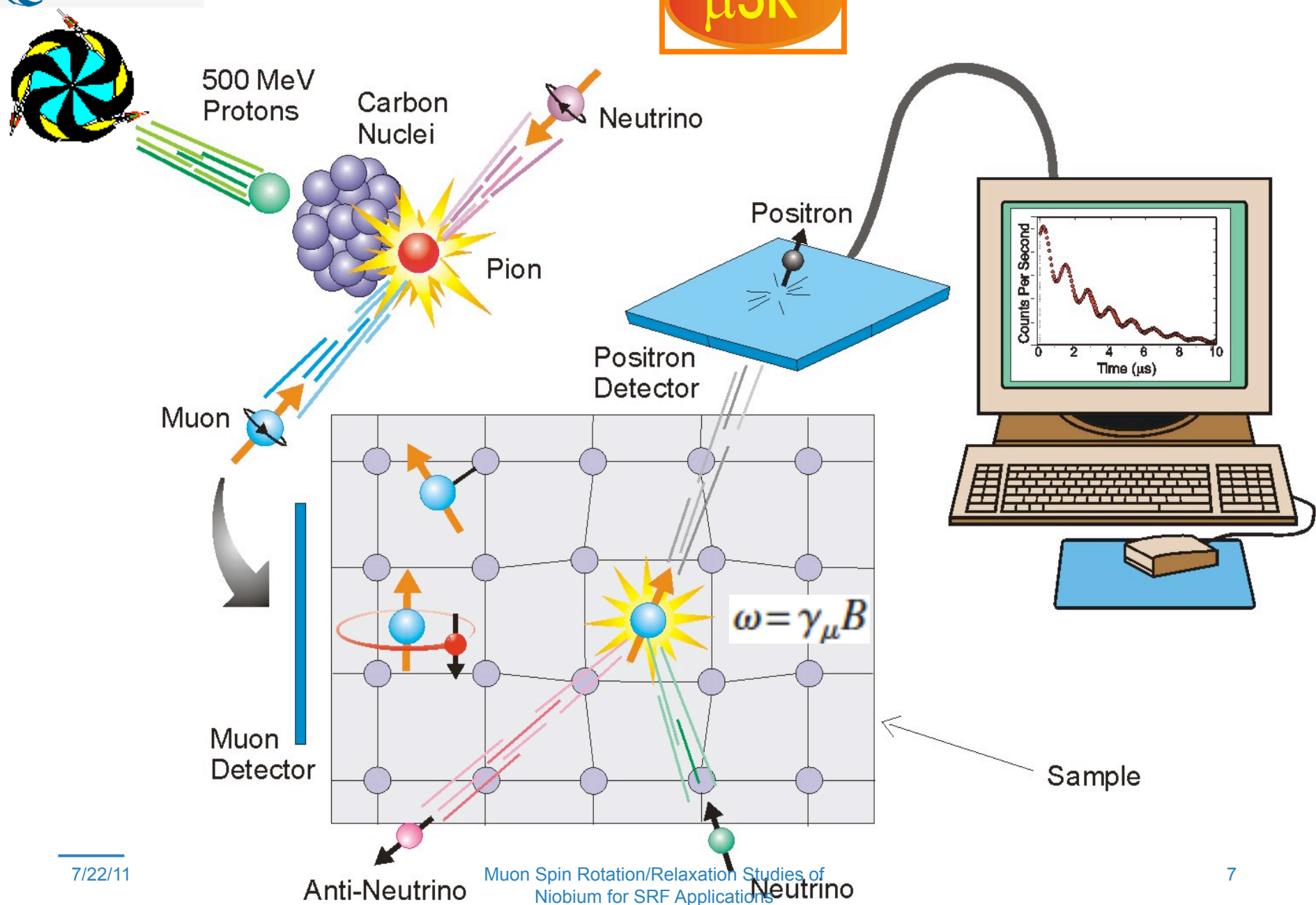
Samples used: cutouts from large/small grain BCP 1.5 GHz cavities (courtesy of Cornell)



7/22/11

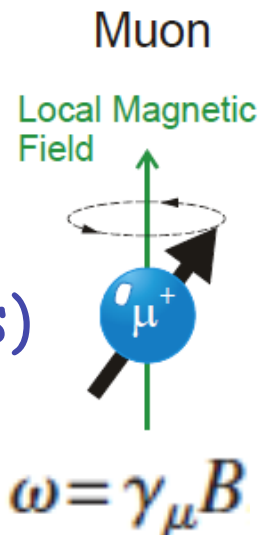


μ SR



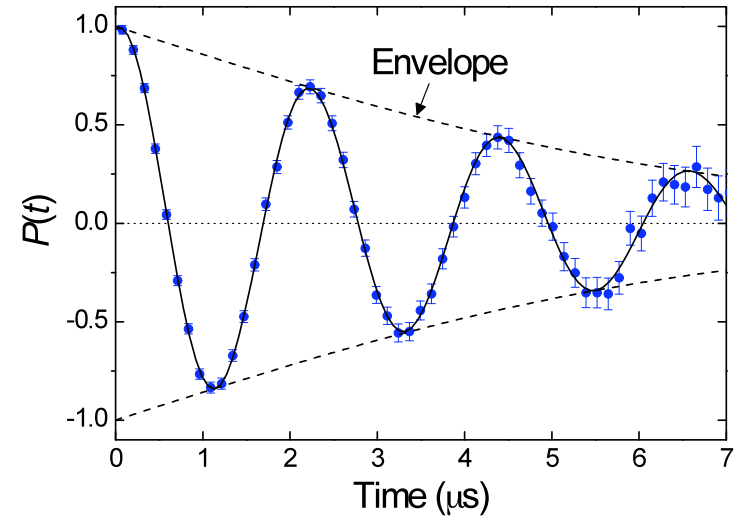
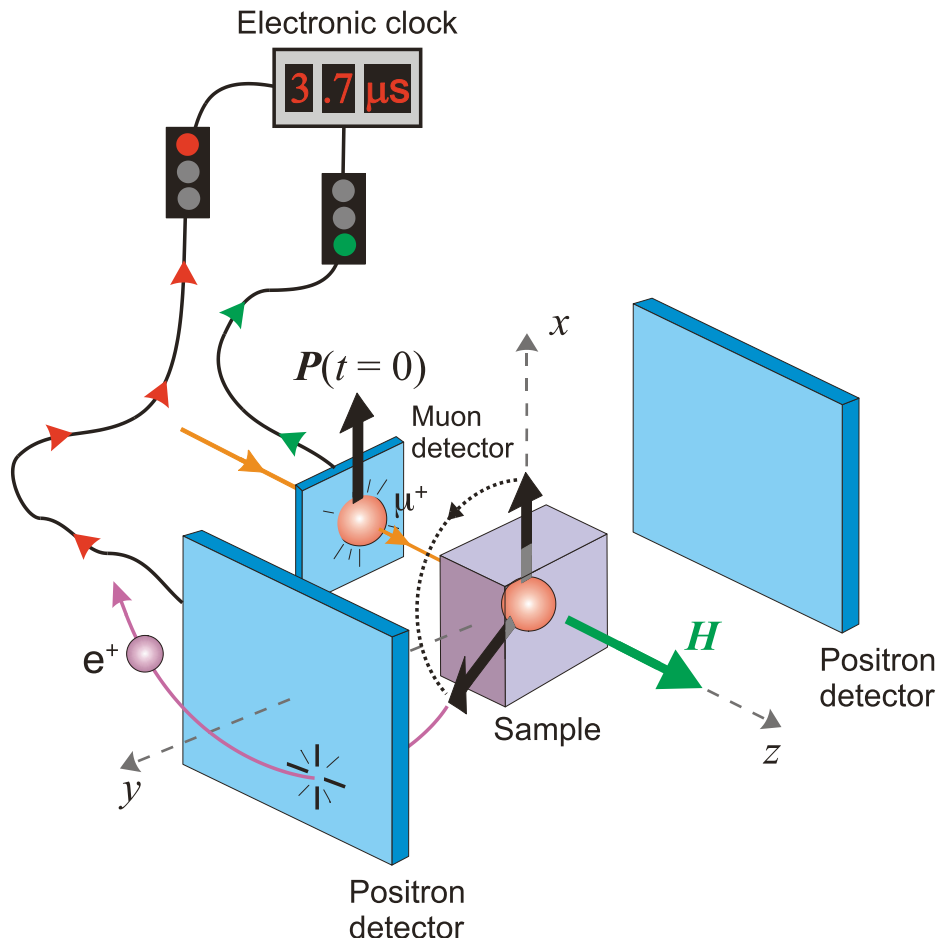
The muon is sensitive to the **vector sum** of the local magnetic fields at its stopping site. The local fields consist of:

- those from **nuclear** magnetic moments
 - those from **electronic** moments
(100-1000 times larger than from nuclear moments)
 - **external** magnetic fields
- As a local probe, μ SR can be used to deduce Magnetic volume fractions
- So we will be able to measure what fraction of the sample is penetrated by magnetic flux as function of the field, and look for correlation with the RF performances



$$\omega = \gamma_\mu B$$

Field of first entry measurement: Transverse-Field μ SR

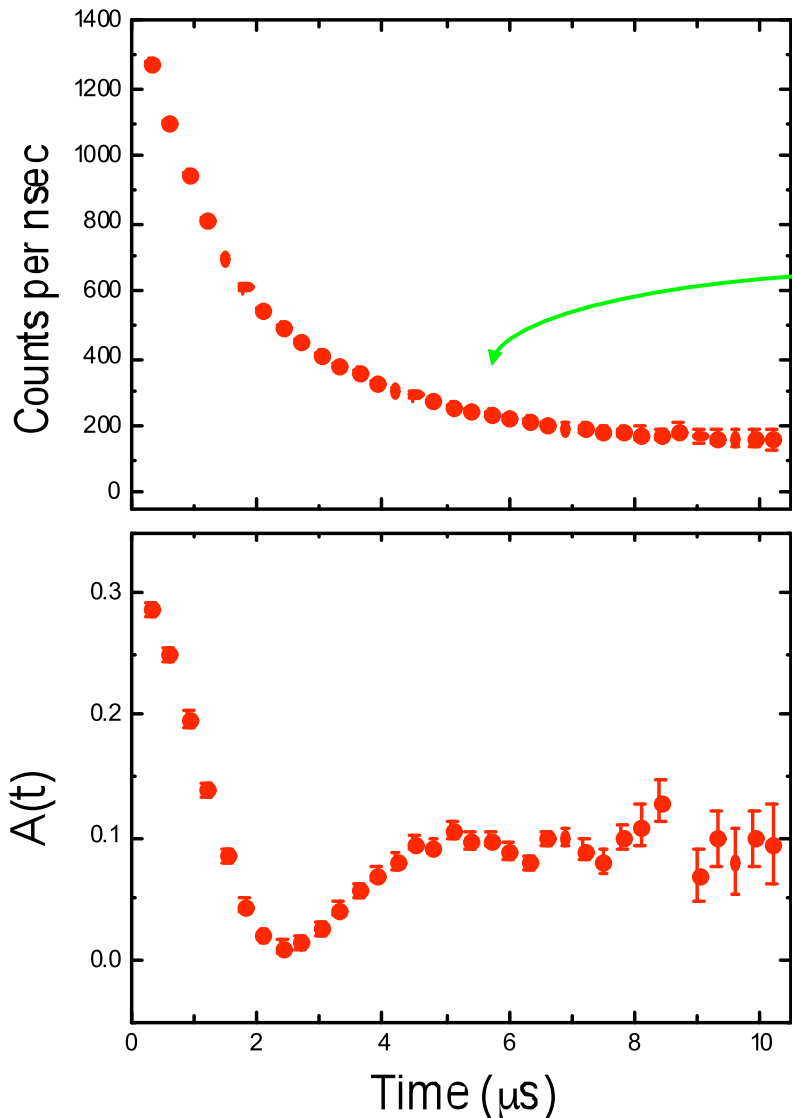


The information on local fields is contained in the time evolution of the muon spin Polarization which is described by:

$$P(t) = G(t) \cos(\gamma_\mu B_\mu t + \phi)$$

where $G(t)$ is a relaxation function describing the **envelope** of the TF- μ SR signal that is sensitive to the width of the static field distribution or temporal fluctuations.

Signal obtained: asymmetry spectrum



The **count rates** for opposing e^+ detectors:

$$N_B(t) = N_0 e^{-t/\tau_\mu} \left[1 + a_0 G(t) \cos(\gamma_\mu B_\mu t + \Phi) \right]$$

$$N_F(t) = N_0 e^{-t/\tau_\mu} \left[1 - a_0 G(t) \cos(\gamma_\mu B_\mu t + \Phi) \right]$$

Forming the B - F count rate ratio:

$$\frac{N_B(t) - N_F(t)}{N_B(t) + N_F(t)} = a_0 G(t) \cos(\gamma_\mu B_\mu t + \Phi)$$

$$= a_0 P(t) \equiv A(t)$$

← **μ SR asymmetry spectrum**

- Frequency of oscillation → amplitude of local field
- Amplitude of asymmetry → magnetic volume fraction

TF-muSR setup for cutout samples studies

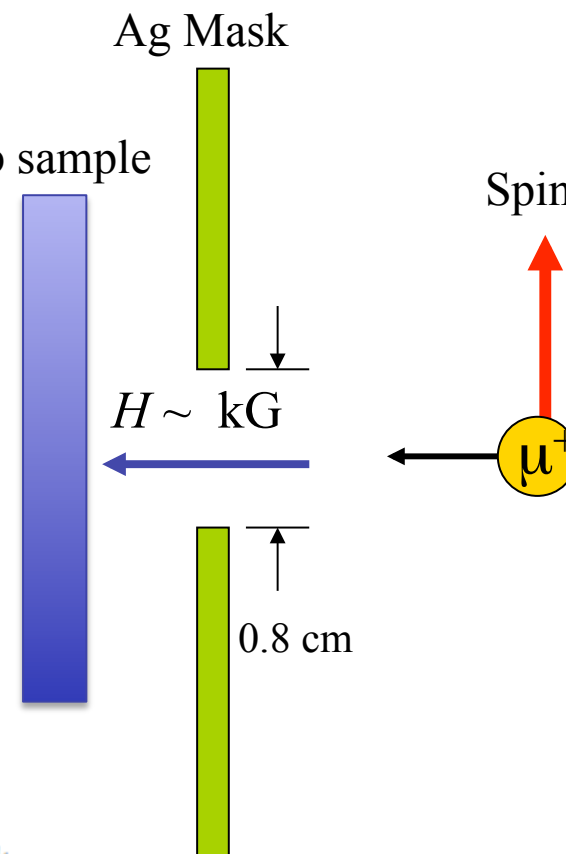
- DC magnetic field perpendicular to sample, T=2.3K (and measurements at 4.5K up to 8K), full scan in field 0-270mT

Samples:

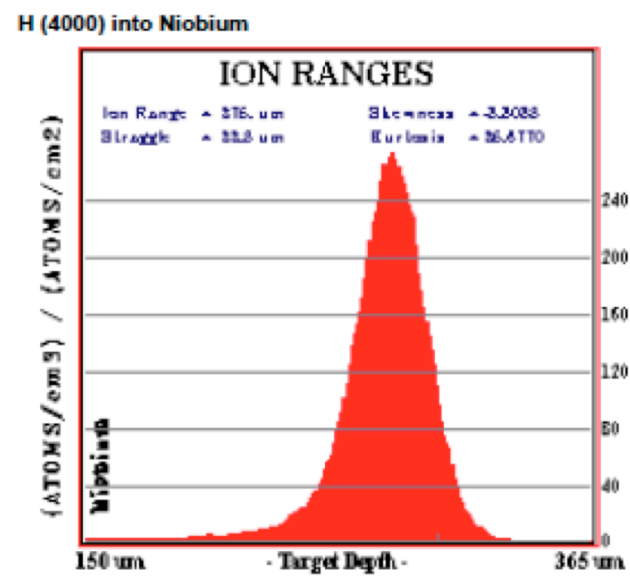
- 3 mm thick Nb sample
- 2cm diameter

- Field at the center ~ applied field (in the field range of interest -above 70mT, $B_y(0,0) \sim 15\text{mT}$ behind

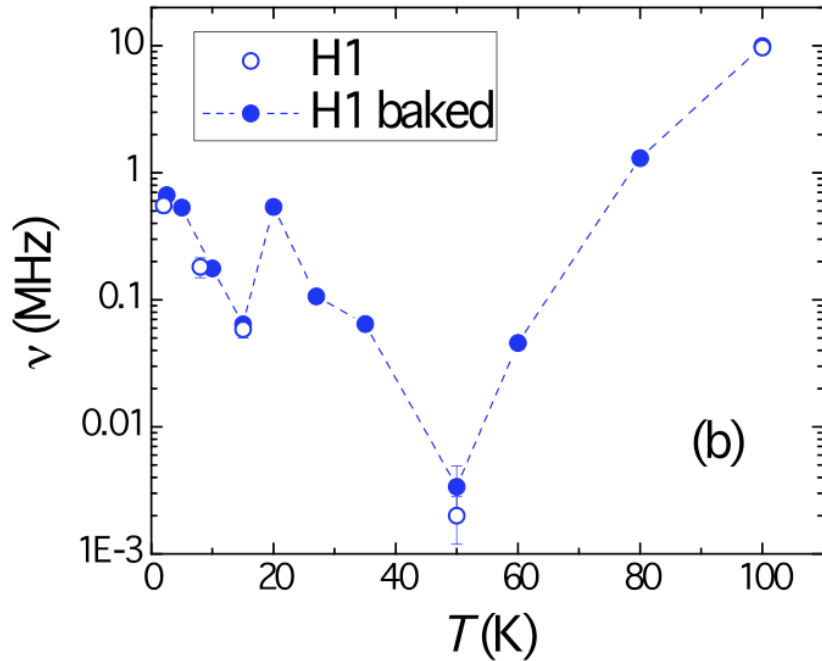
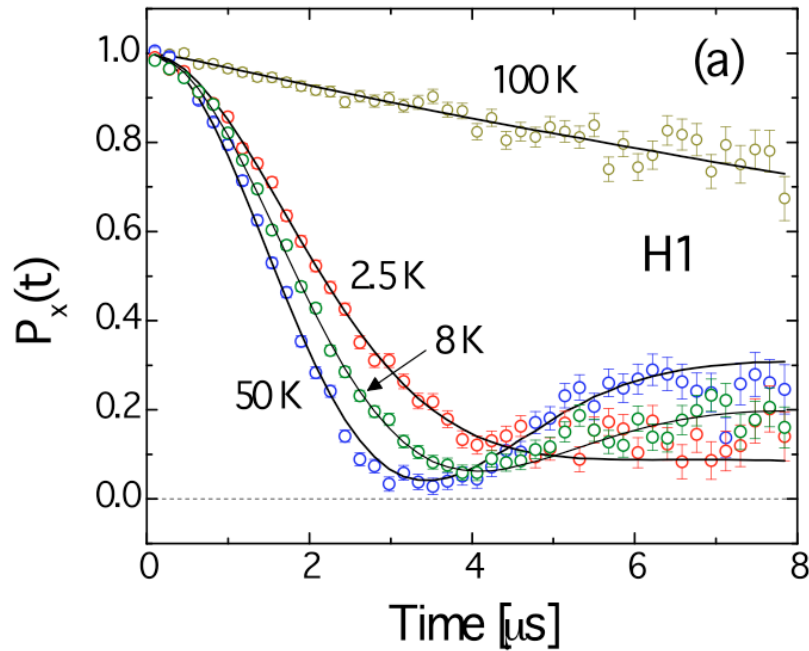
B_{appl}) Ernst Helmut Brandt
Irreversible magnetization of pin-free type-II superconductors PHYSICAL REVIEW B VOLUME 60, NUMBER 17



Muon stopping depth $\sim 300\mu\text{m}$



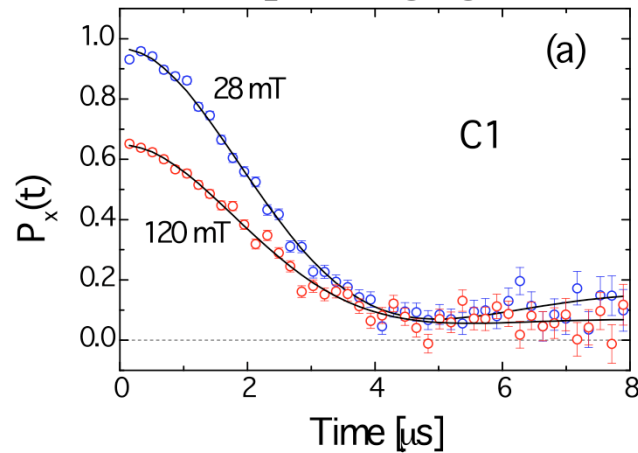
Zero Field muSR results



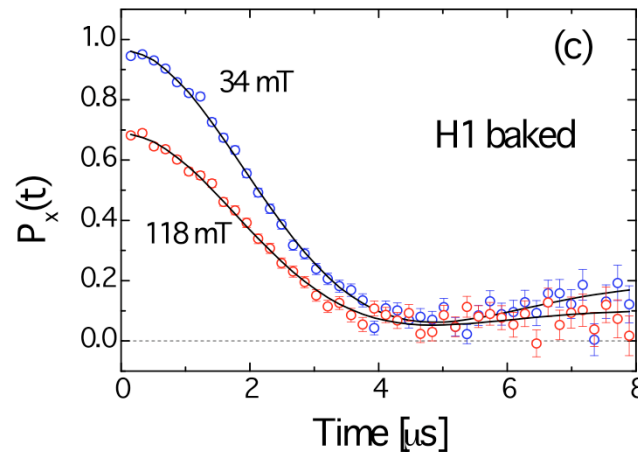
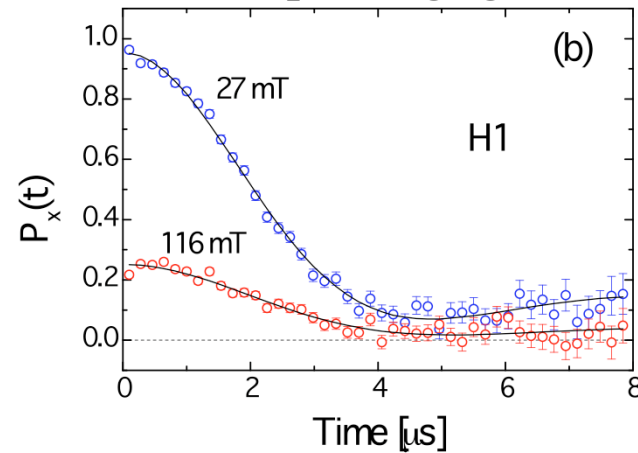
- Representative ZF- μ SR spectra of sample H1 at different temperatures, which depends on lattice properties and impurity content
- Temperature dependence of the muon hop rate in sample H1 before and after baking
- Results consistent with what observed in previous μ SR experiments on nitrogen doped Nb
- **Measurement very interesting to be done in the surface layer to study hydrogen trapping at the surface before/after baking**

Example of asymmetry signals, 30 and 120mT, 2.3K

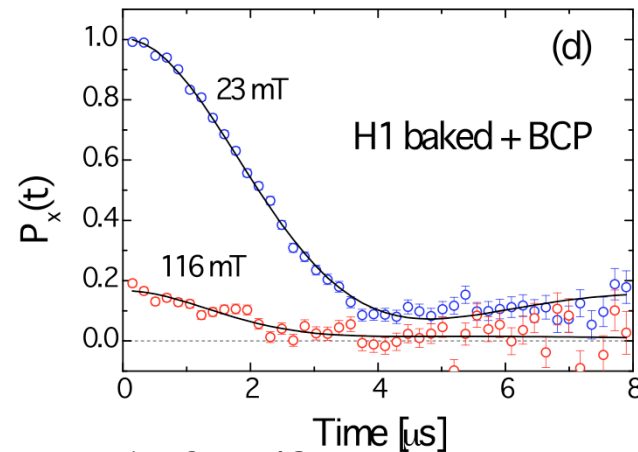
C1- cold spot large grain cutout,



H1 – hot spot large grain cutout

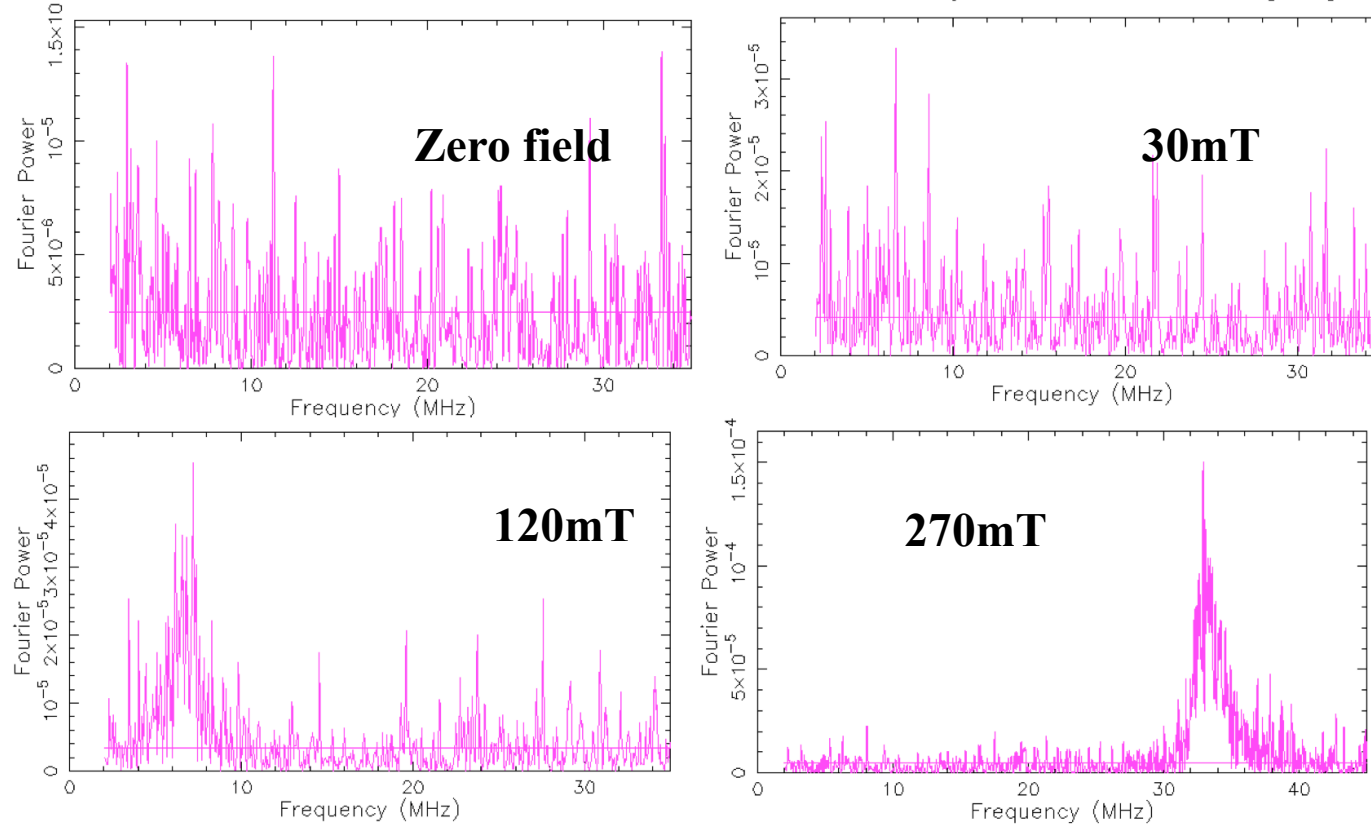


**H1 after 48 hours UHV
120C baking**



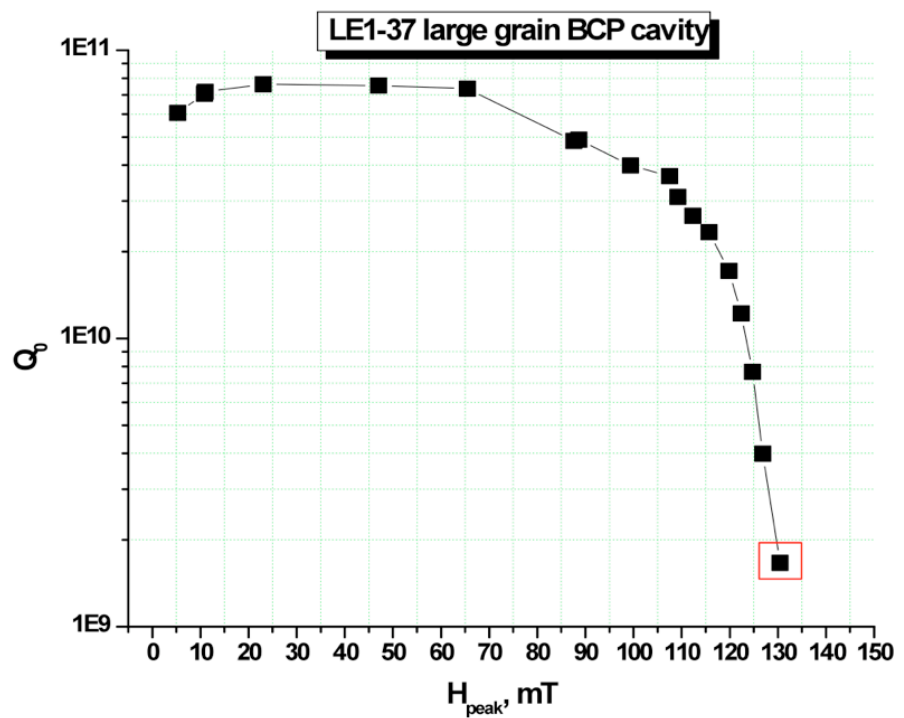
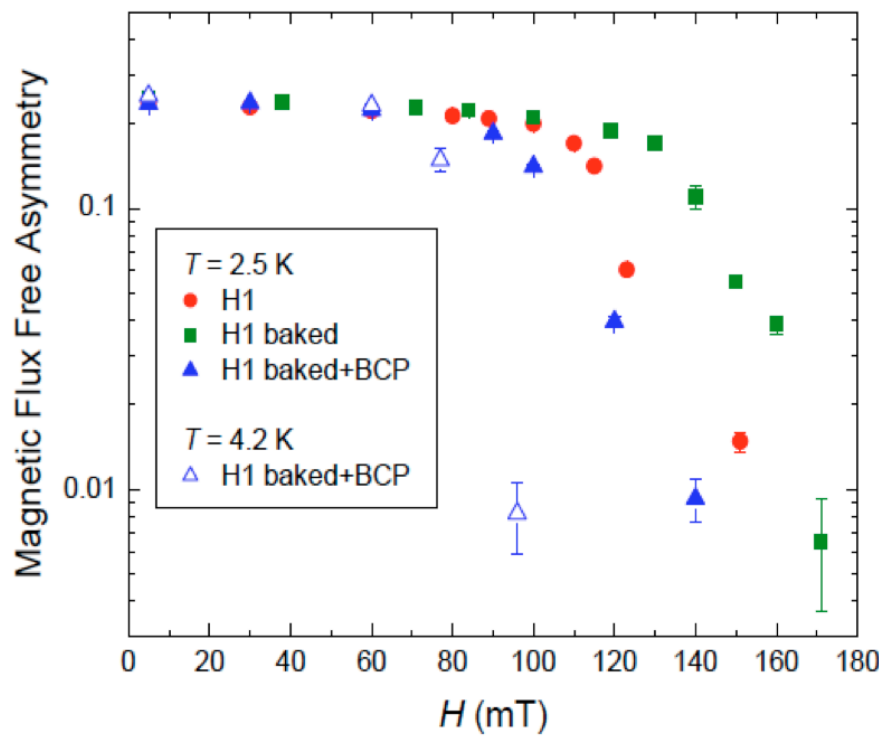
**H1 after 48 hours UHV
120C baking plus 5 μ m BCP**

Fast Fourier Transform: internal field distribution



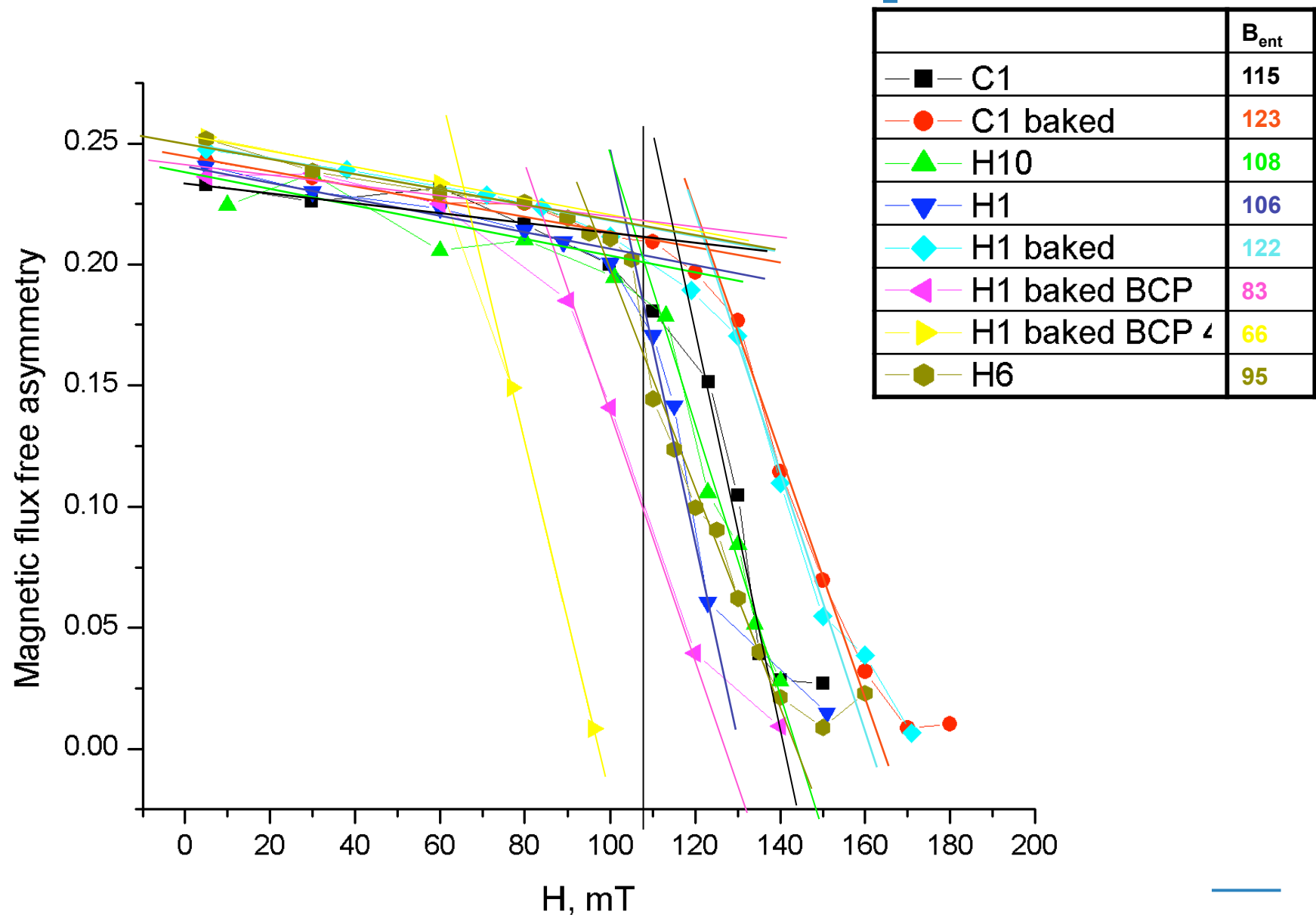
Fast Fourier transforms for sample H1 at 2.3K and respectively field levels: zero, 30mT, 120mT (peak of flux appearing at ~ 50 mT), 270mT (peak of flux ~ 260 mT)
→ Suggests an inhomogeneous surface with preferential sites for flux entry

Strong correlation fraction of sample NOT containing flux vs RF cavity performance

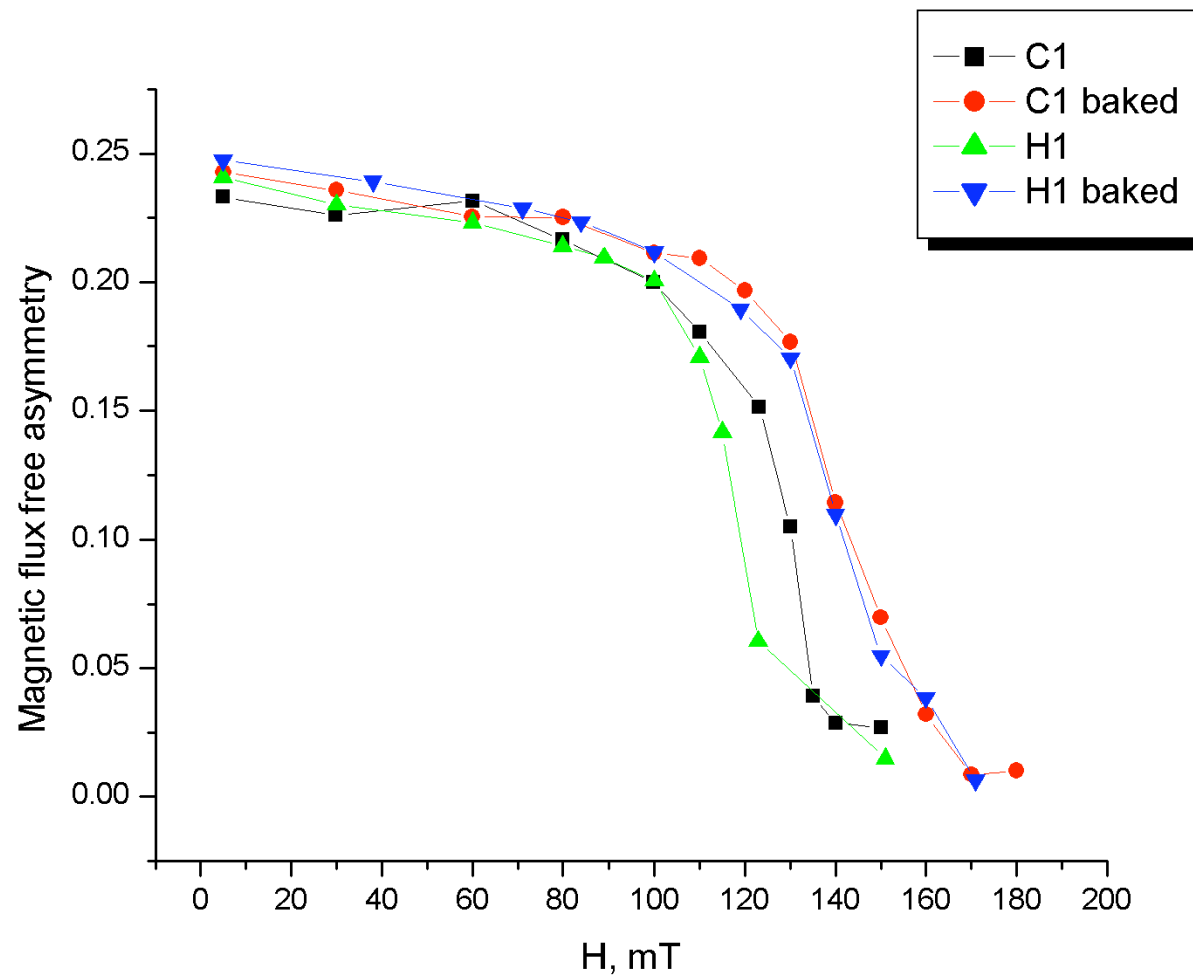


- Onset of flux entry measured with muSR strongly correlates with onset of RF HF losses as for thermometry characterization
- Measurements consistent among all 6 samples tested

Results - all samples



Hot vs Cold sample before/after bake



In conclusion

- Muon spin rotation used @ TRIUMF for SRF applications for the first time
- Experiment results strongly suggest early magnetic flux entry at ‘weaker spots’ as high field Q-slope losses mechanism in SRF Nb cavities
- Invaluable tool for studying superconducting parameters (λ , ξ , H_{c1} , H_{c2} ...) and their temperature/field dependence

Future direction

- First establish **baseline**: study **ultrapure Nb** single crystal (field of entry, superconducting parameters)
- Understand **which step of Nb processing for cavities causes early flux entry** → systematic study of field of entry for niobium with different treatments, degree of cold work, RRR...
- **Q_0 and medium field losses** studies: design apparatus for parallel field measurements
- Study **quench and post baking losses** spots (Romanenko, FNAL)
- **Thin films and multilayer**: accurate tool for field of entry
- Beamtime already approved for these studies, to be scheduled in fall
- **LEM** for penetration depth and role of hydrogen in surface

Thanks for your attention!

Back up slides

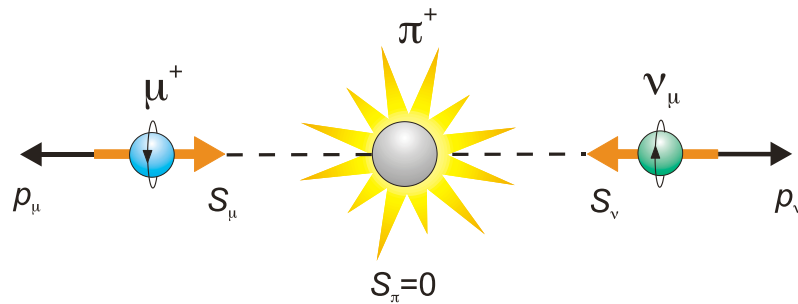
Pion Decay: $\pi^+ \rightarrow \mu^+ + \nu_\mu$

A pion resting on the downstream side of the primary production target has zero linear momentum and zero angular momentum.

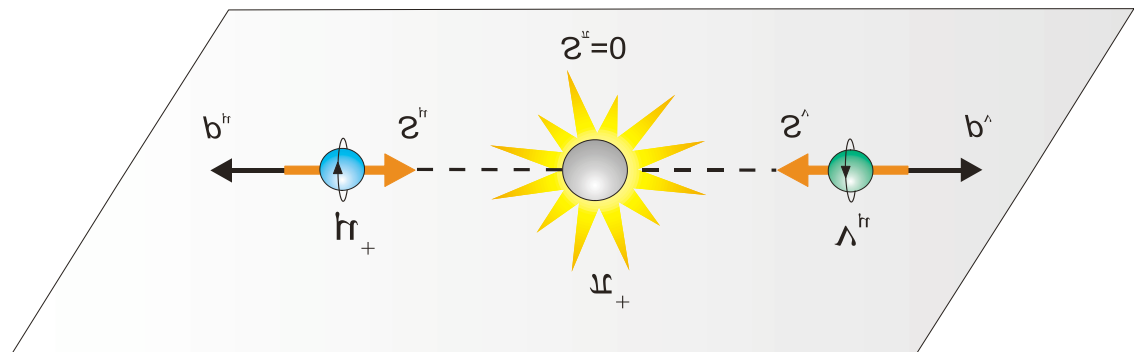
Conservation of Linear Momentum: μ^+ emitted with momentum equal and opposite to that of the ν_μ

Conservation of Angular Momentum: μ^+ and the ν_μ have equal and opposite spin

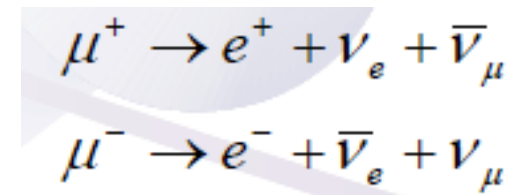
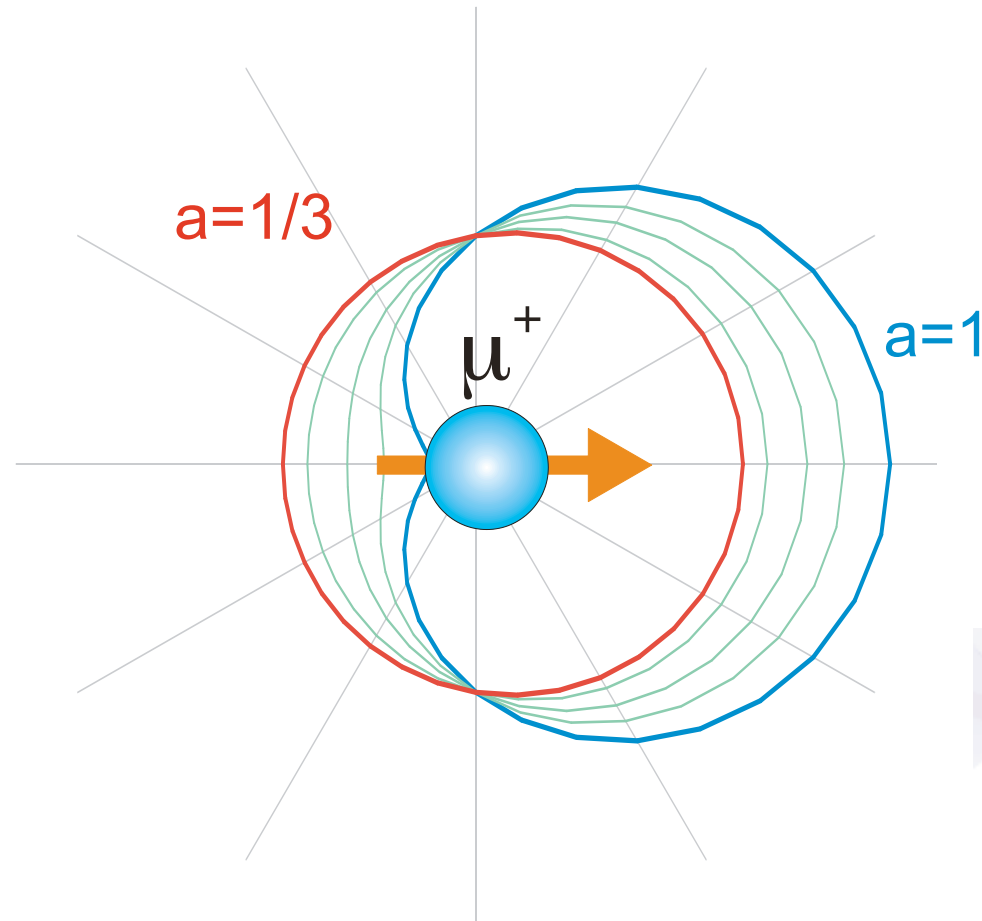
Weak Interaction: only “left-handed” ν_μ are created. **Therefore the emerging μ^+ has its spin pointing antiparallel to its momentum direction**



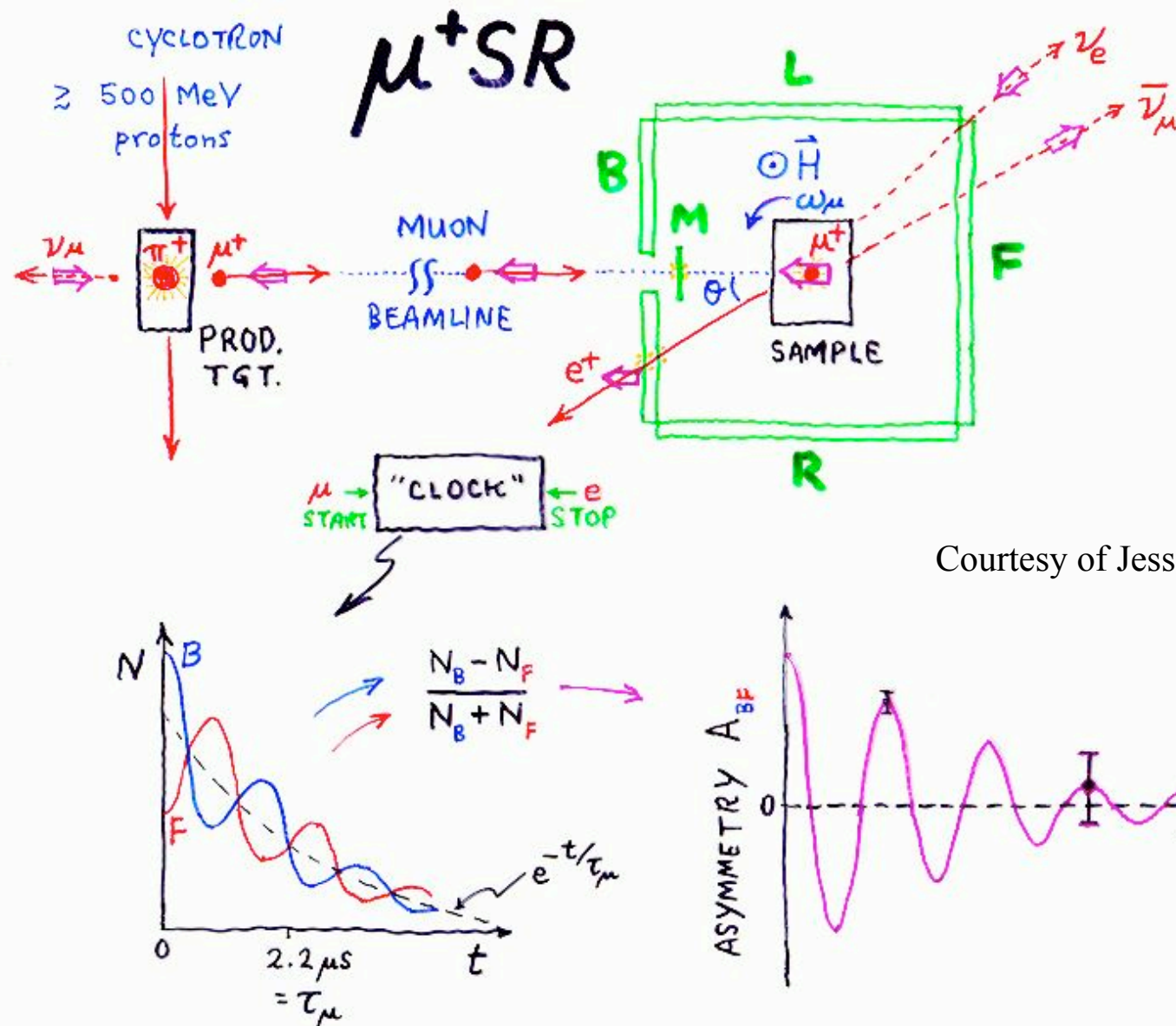
→ 100% spin polarized!



μ^+ -Decay Asymmetry

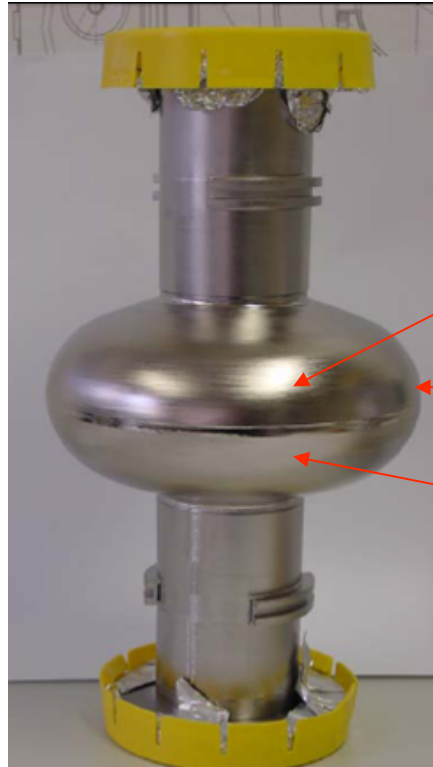


Angular distribution of positrons from the μ^+ -decay. The asymmetry is $a = 1/3$ when all positron energies are sampled with equal probability.

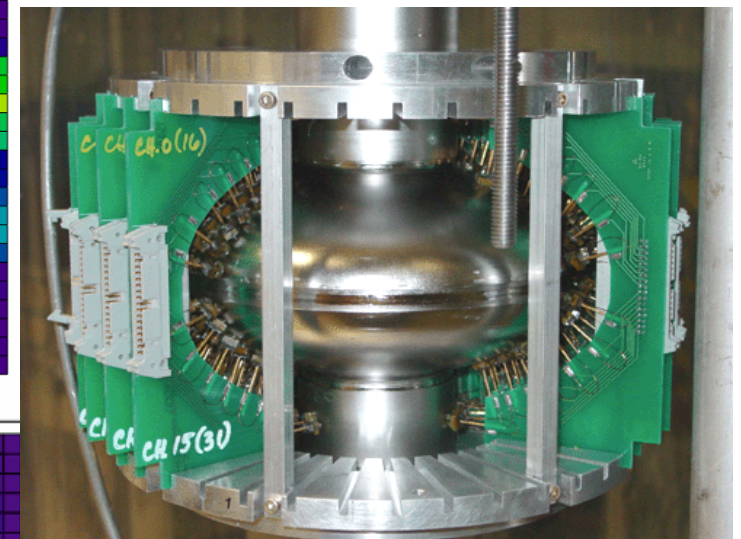
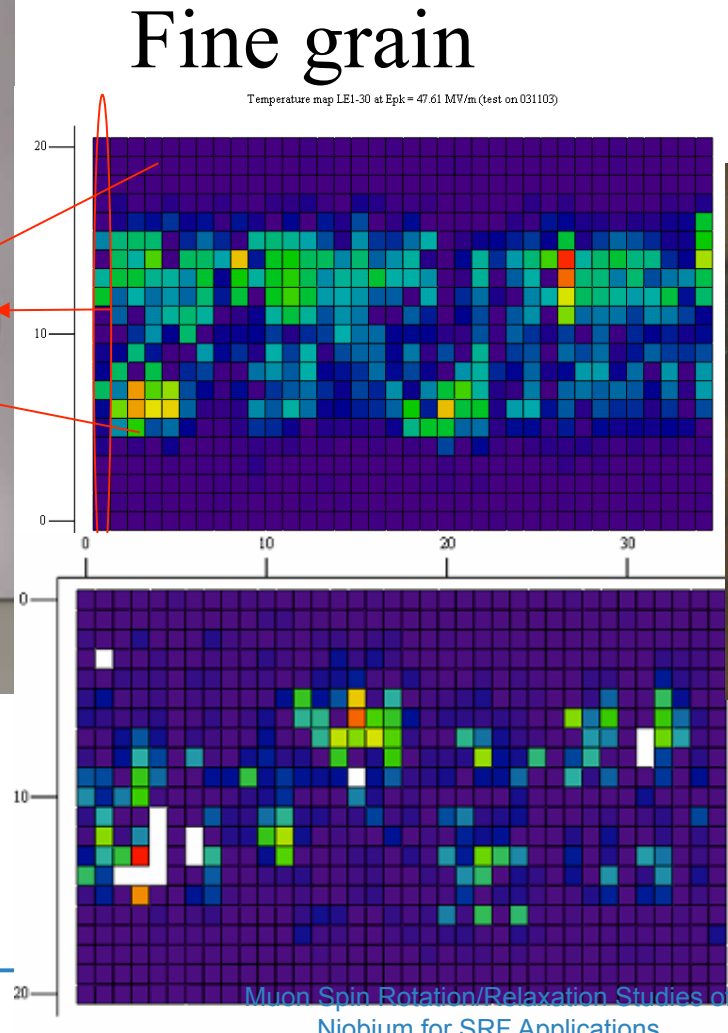


Courtesy of Jess Brewer, TRIUMF

Thermometry characterization of losses

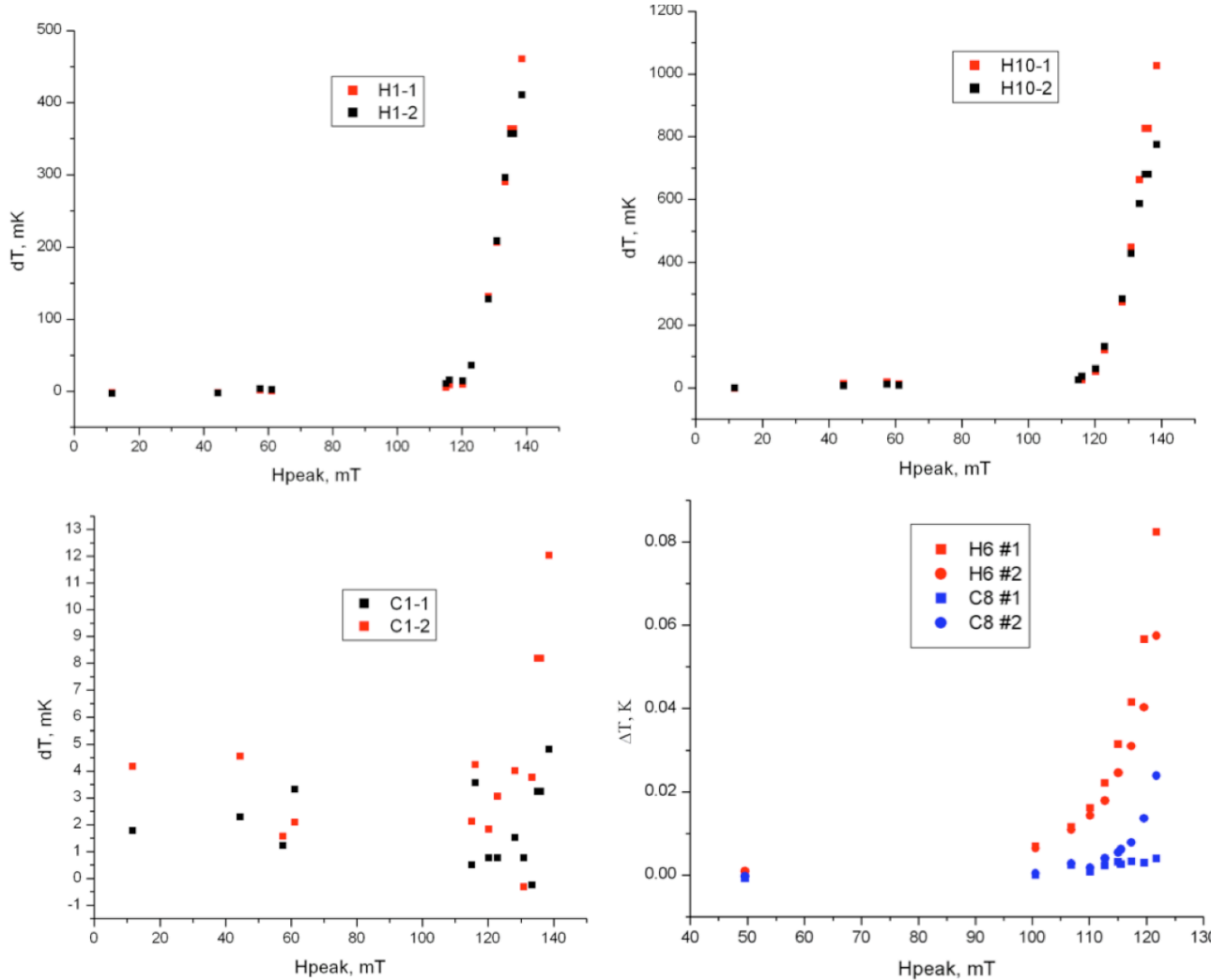


Large grain

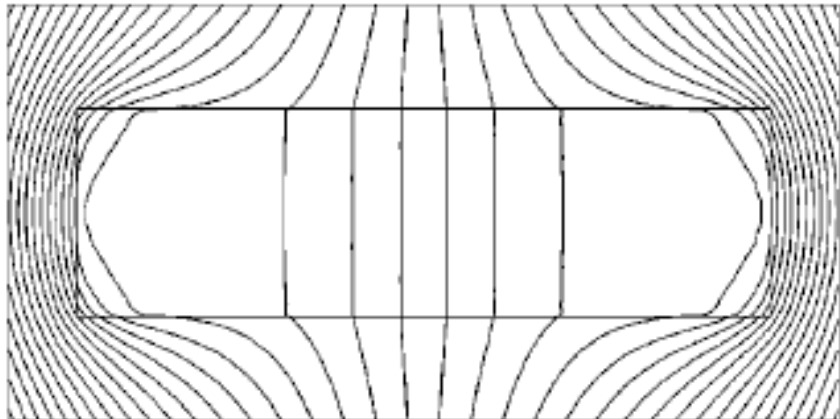


Example of T-map system, G.Ciovati
Ph.D. thesis

RF characterization of samples studied (A.Romanenko)



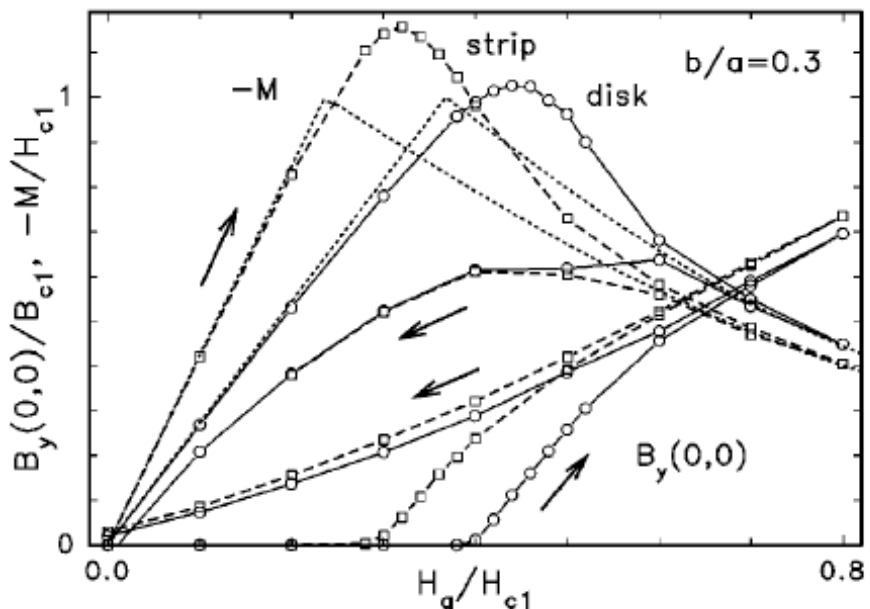
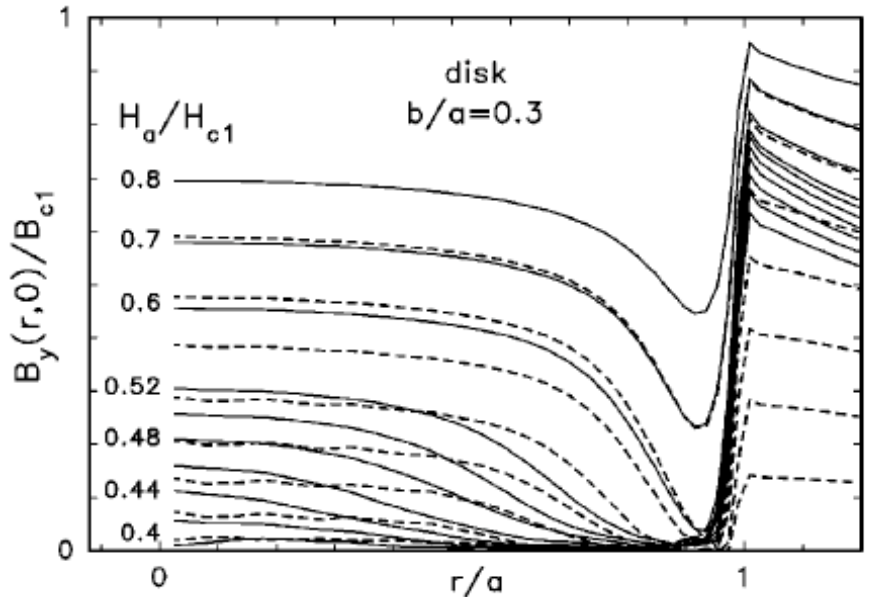
Brandt – demagnetization

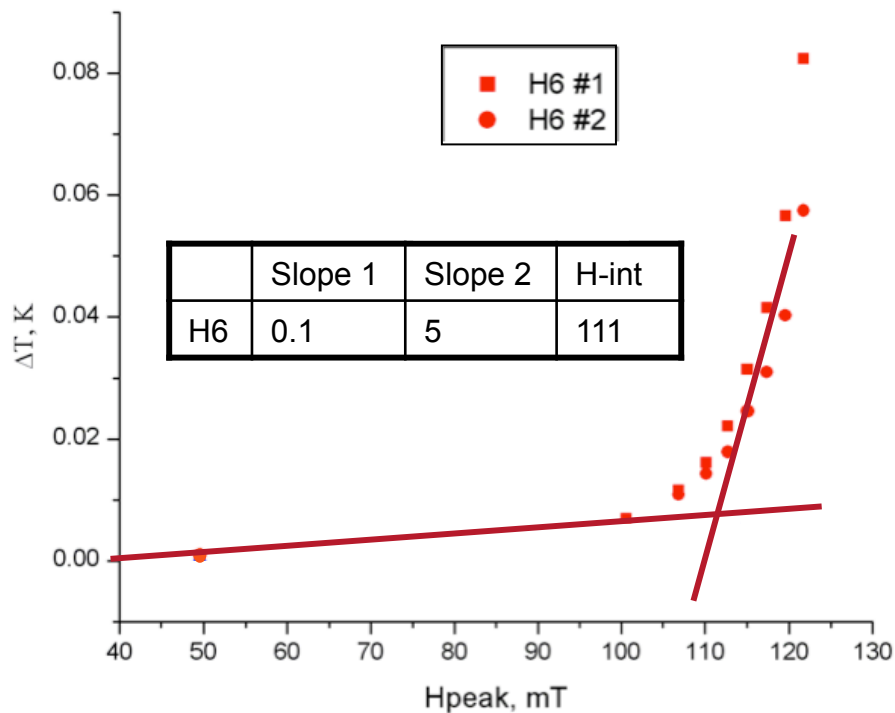
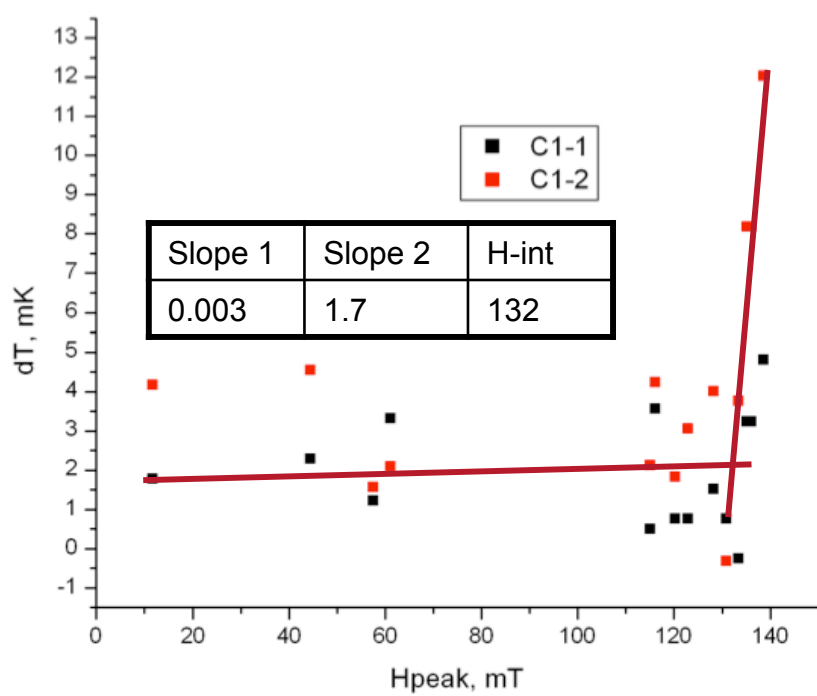
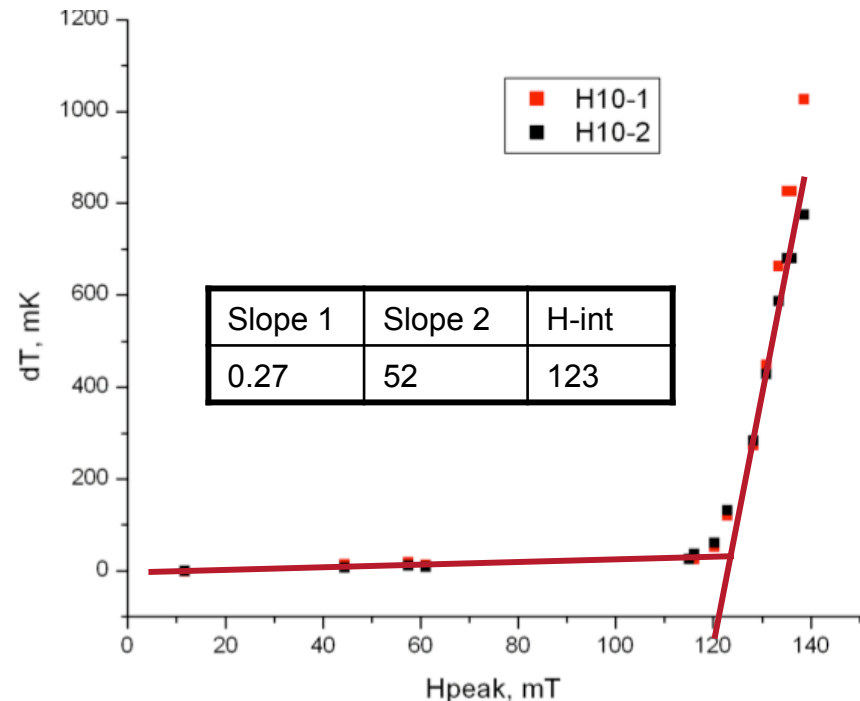
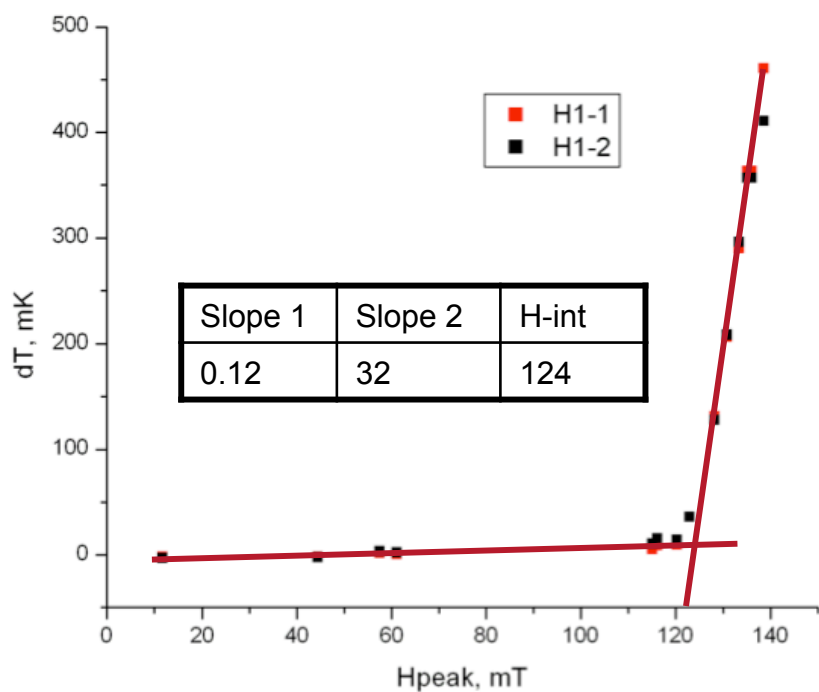


$$H_{\text{en}}^{\text{strip}}/H_{c1} = \tanh \sqrt{0.36b/a},$$

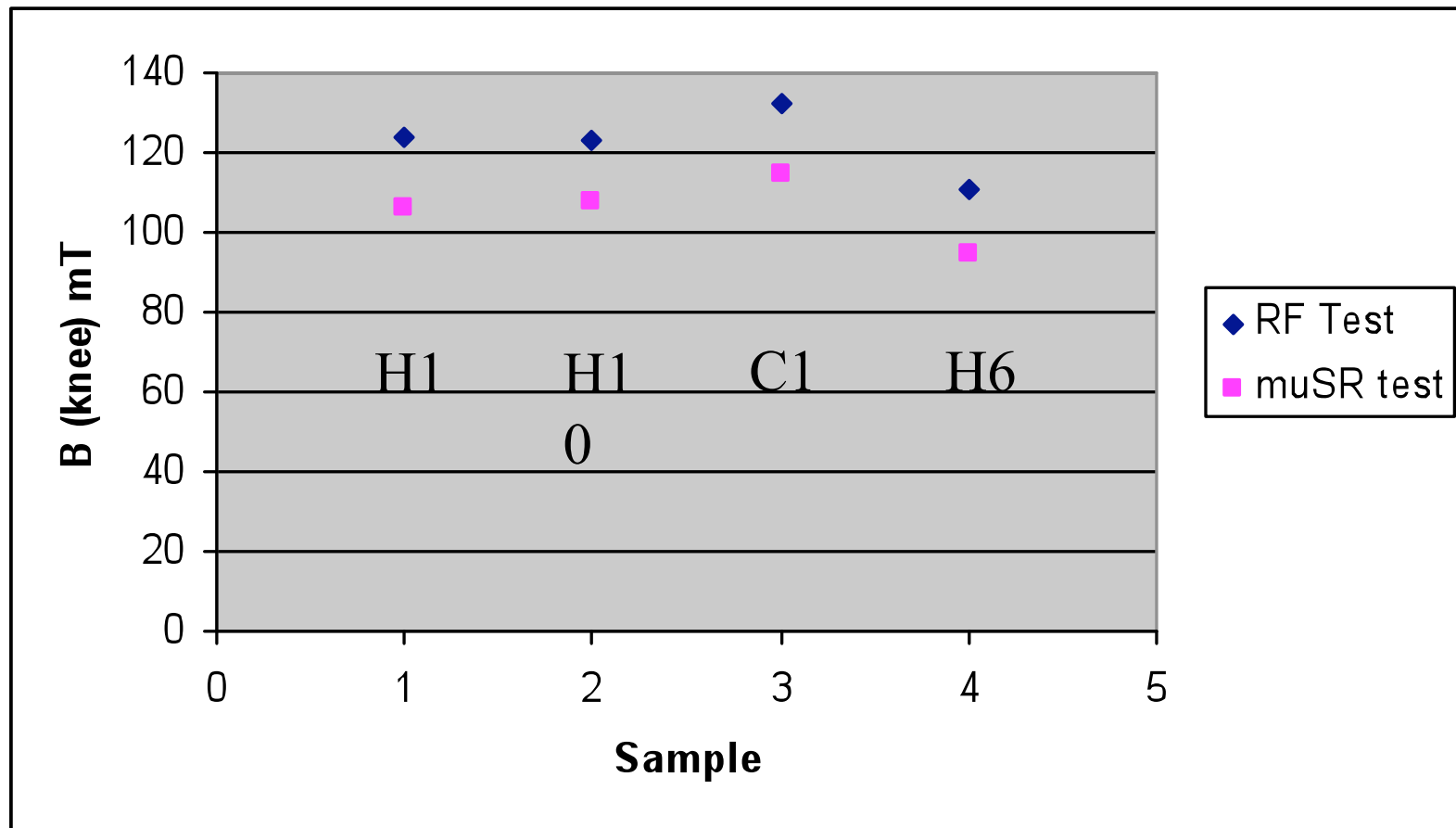
$$H_{\text{en}}^{\text{disk}}/H_{c1} = \tanh \sqrt{0.67b/a}.$$

Ernst Helmut Brandt
 Irreversible magnetization of pin-free type-II superconductors
 PHYSICAL REVIEW B VOLUME 60, NUMBER 17





Knee points (RF heating vs field entry)



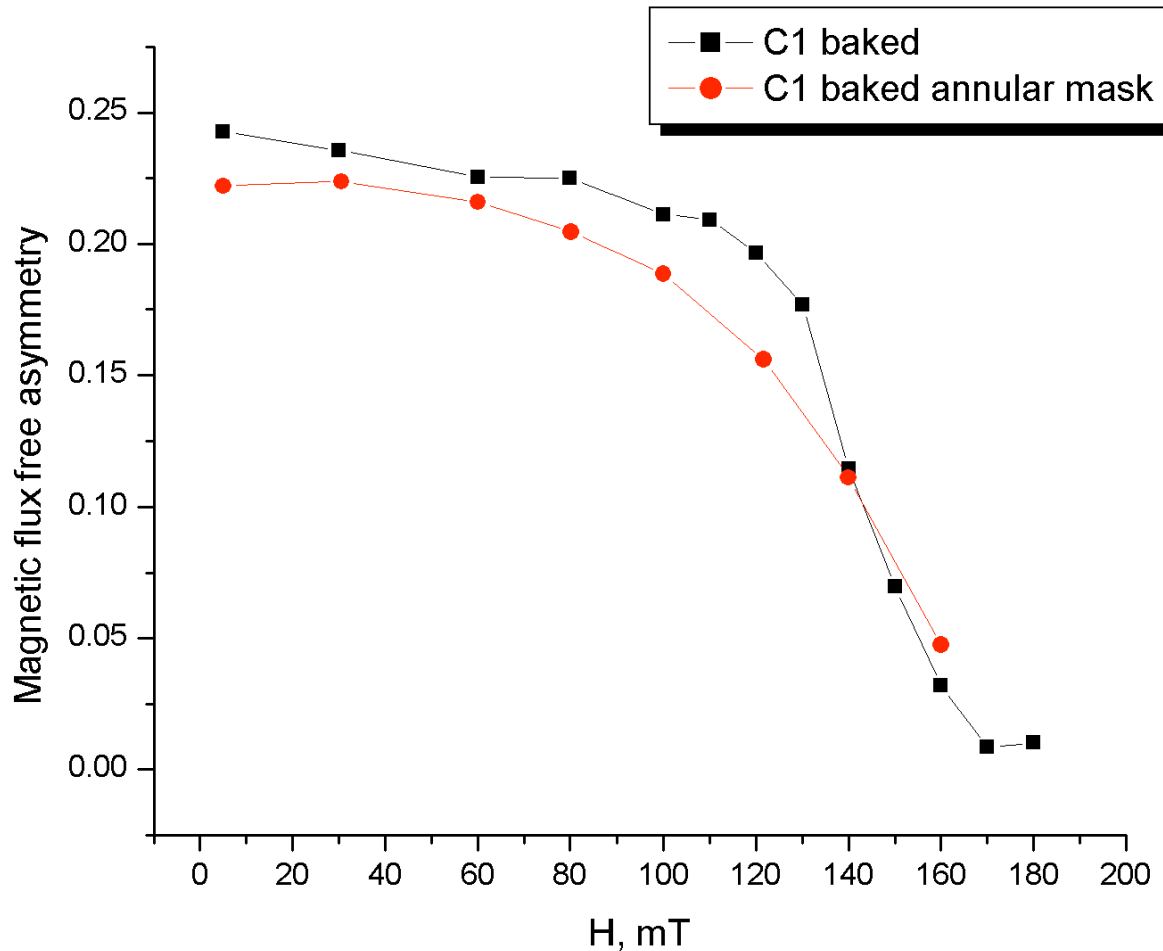
$$\Delta B = 16 \text{ mT} \pm 1.5 \text{ mT}$$

Processing

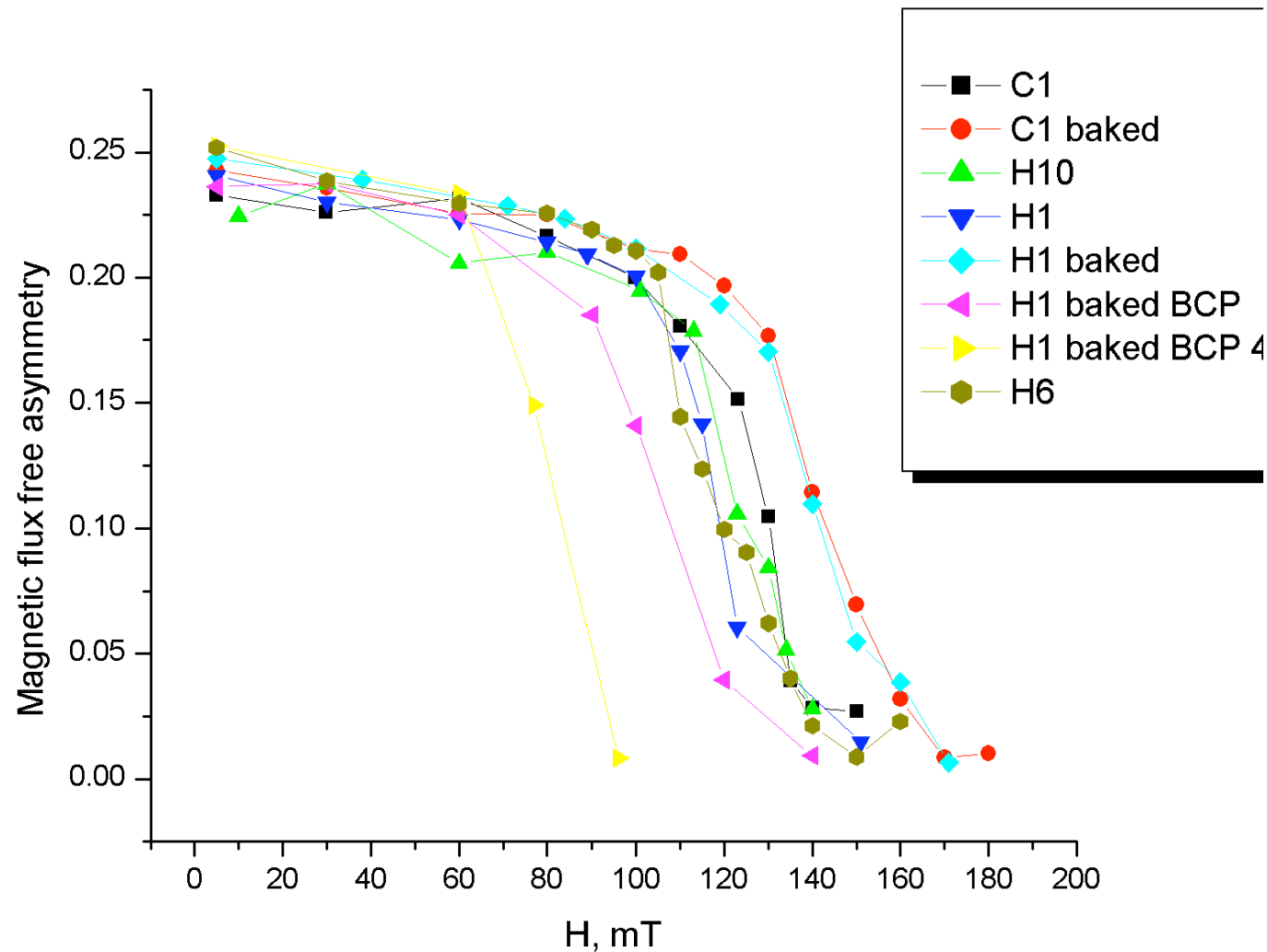
	musR	~RF	T	Brf (T=0)	BmuSR (T=0)
H1	106	122	2.3	130.13	113.07
H1baked	122	138	2.3	147.20	130.13
H1baked+BCP	83	99	2.3	105.60	88.53
H1baked+BCP @4.5K	66	82	4.5	107.79	86.76

$$H_c(T) = H_c(0) \cdot \left[1 - \left(\frac{T}{T_c} \right)^2 \right]$$

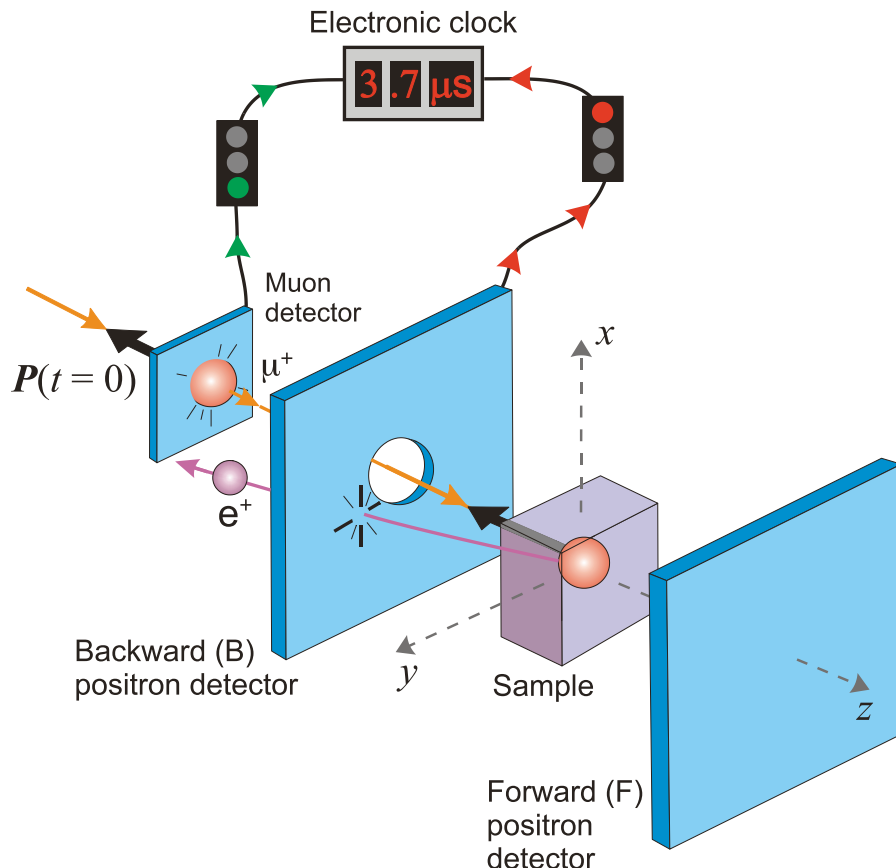
Center vs Annular mask



All samples results



Zero-Field μ SR: internal field distribution, magnetic impurities, trapped flux



The **count rates** for opposing e^+ detectors:

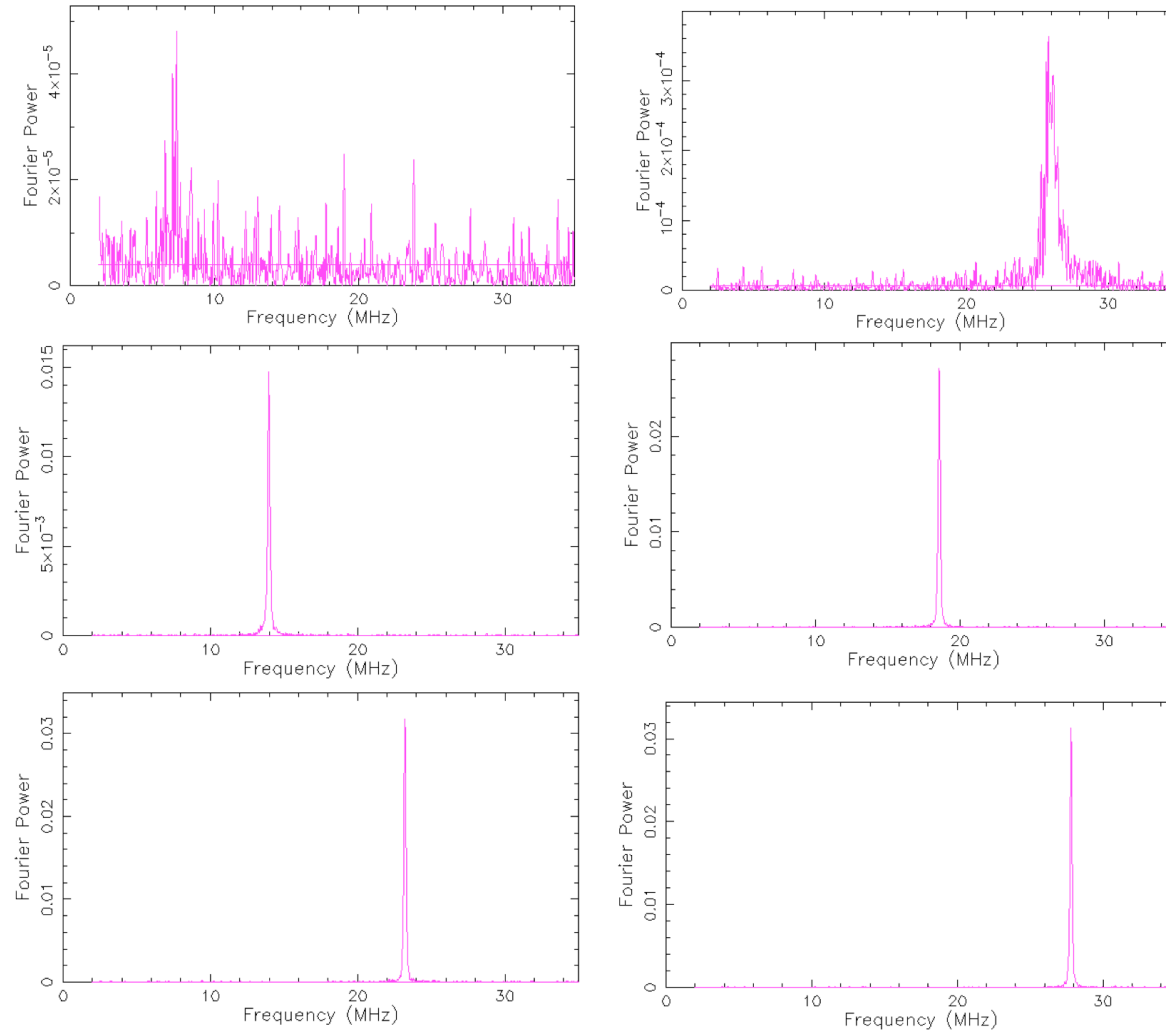
$$N_B(t) = N_0 e^{-t/\tau_\mu} \left[1 + a_0 G(t) \cos(\gamma_\mu B_\mu t + \Phi) \right]$$

$$N_F(t) = N_0 e^{-t/\tau_\mu} \left[1 - a_0 G(t) \cos(\gamma_\mu B_\mu t + \Phi) \right]$$

The corresponding μ^+ spin relaxation function is known as the **Kubo-Toyabe function**

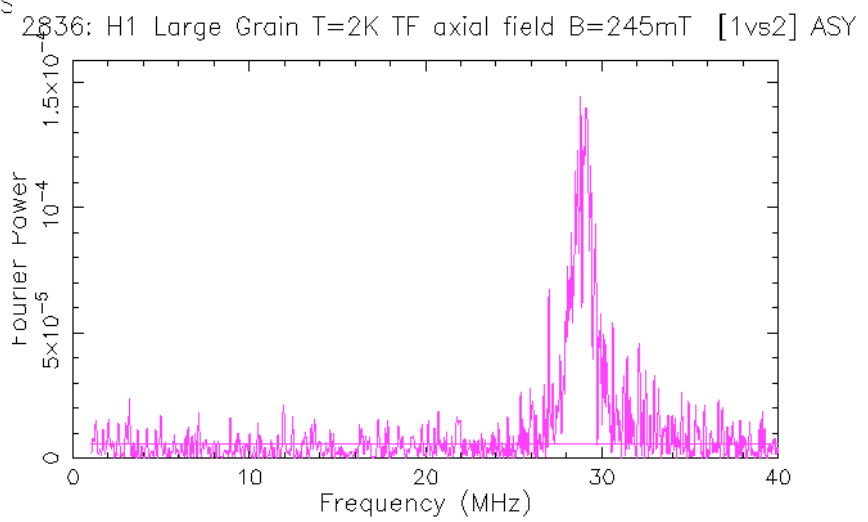
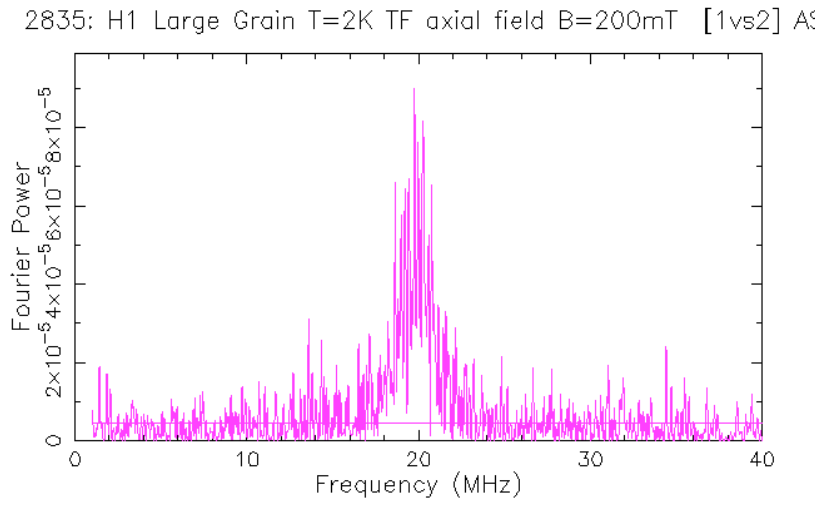
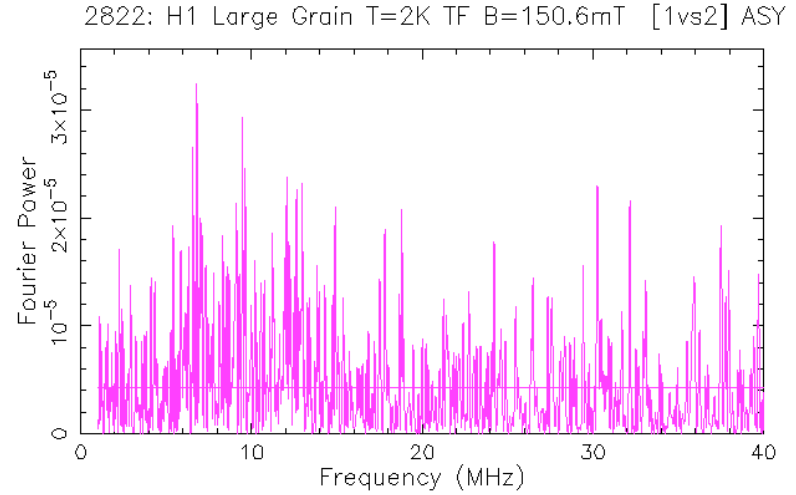
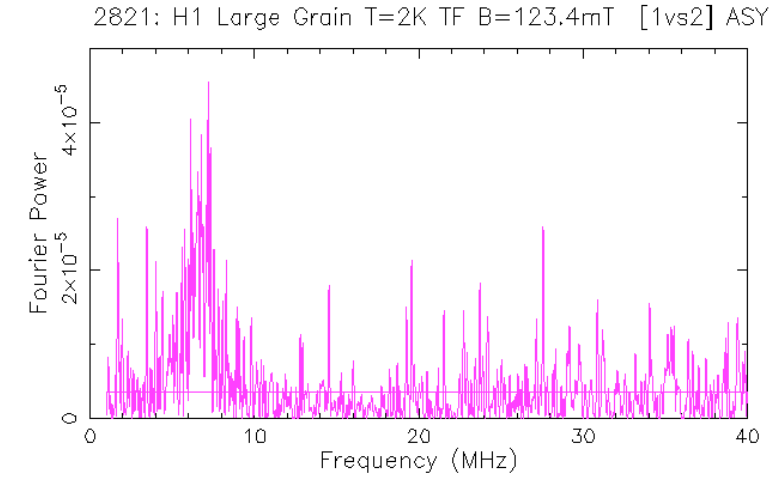
$$G_z(t) = \frac{1}{3} + \frac{2}{3} \left(1 - \Delta^2 t^2 \right) \exp\left(-\frac{1}{2} \Delta^2 t^2\right)$$

Upper critical field measurement

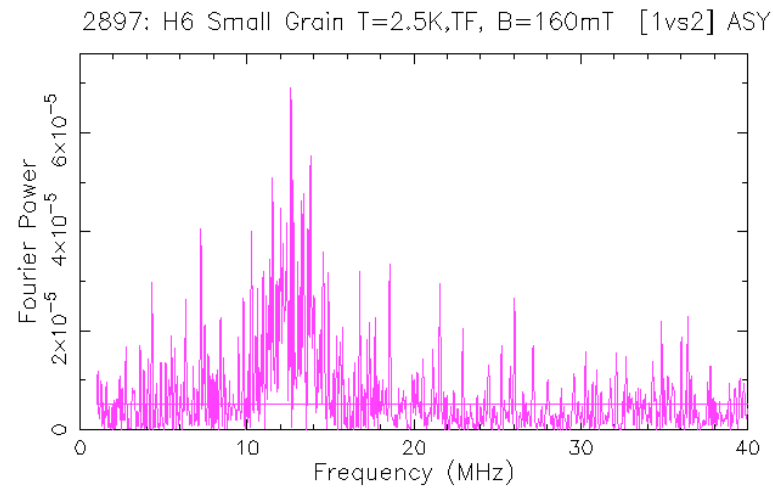
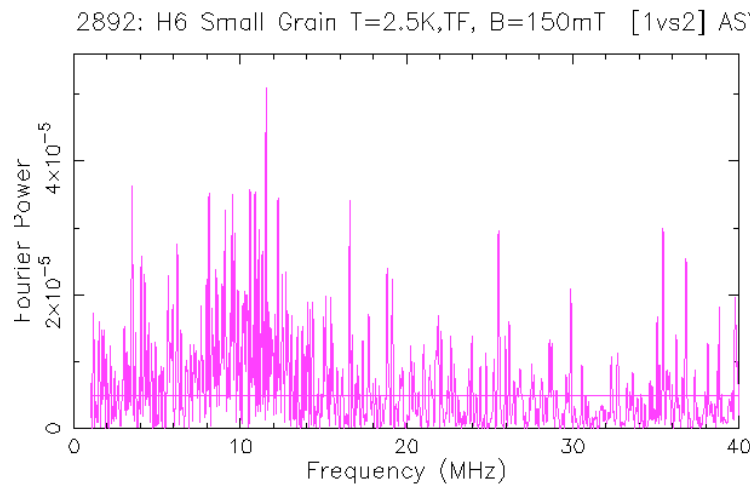
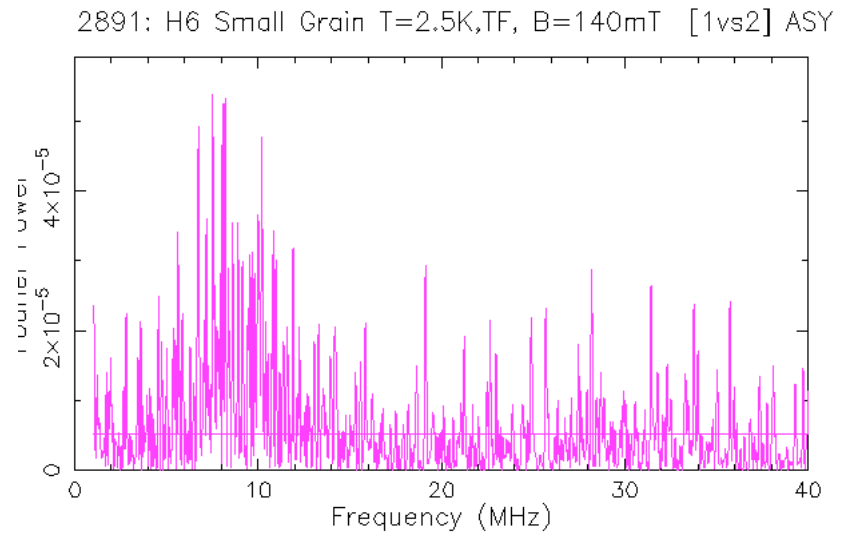
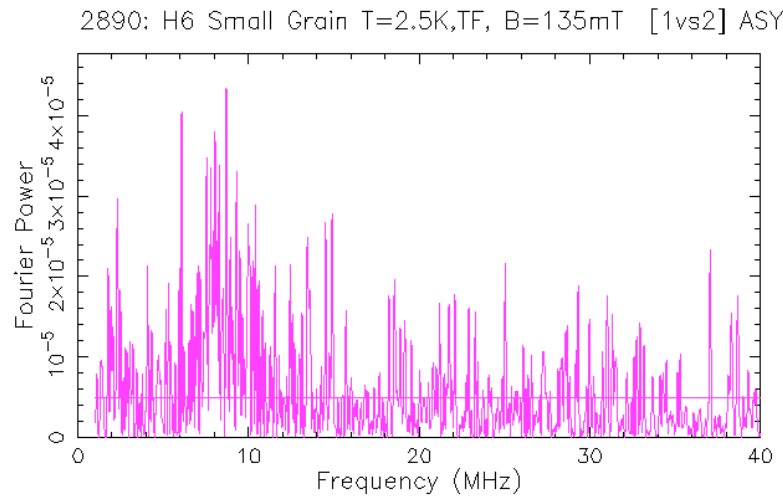


**FFTs for sample H10
respectively for
temperature and fields:
(2.3K, 130mT), (4.5K,
200mT), (7.5K, 100mT),
(7.5K, 140mT), (7.5K,
170mT), (7.5K, 200mT)**

Coexistence of different ‘superconducting’ regions?



Coexistence of different ‘superconducting’ regions?



Nuclear Dipolar Relaxation

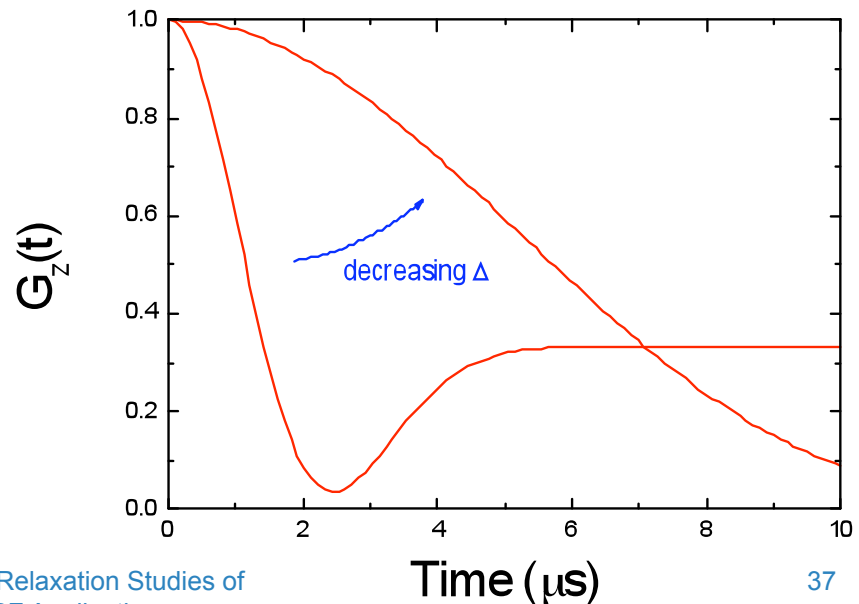
Nuclei with electric quadrupole moments (such as Cu and Y in $\text{YBa}_2\text{Cu}_3\text{O}_{6+x}$) exert an effective dipolar field B_{dip} on the μ^+ . The static (in the $\mu^+\text{SR}$ time window) internal fields are Gaussian distributed in their values and randomly oriented

$$n(B_i) = \frac{1}{\sqrt{2\pi}} \frac{\gamma_\mu}{\Delta} \exp\left(-\frac{1}{2} \frac{\gamma_\mu^2 B_i^2}{\Delta^2}\right) \quad (i = x, y, z)$$

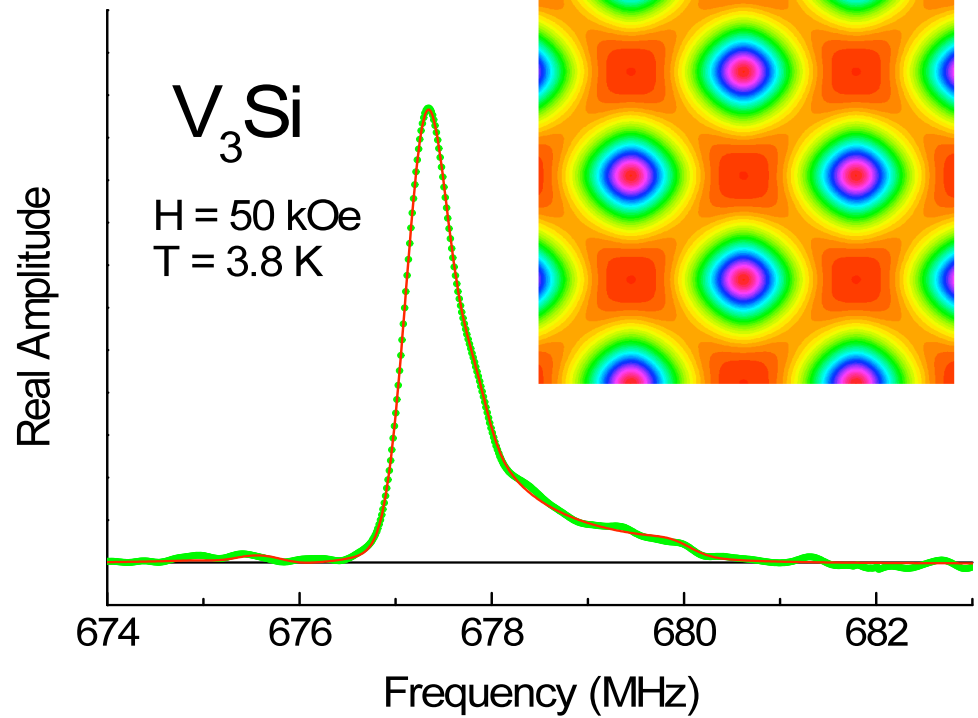
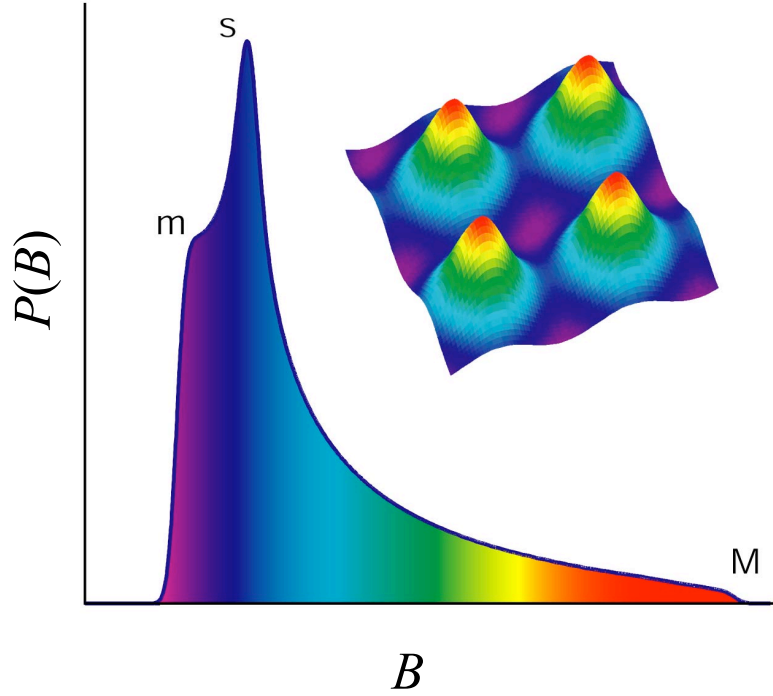
where Δ^2/γ_μ^2 is the second moment of the field distribution

The corresponding μ^+ spin relaxation function is known as the **Kubo-Toyabe function**

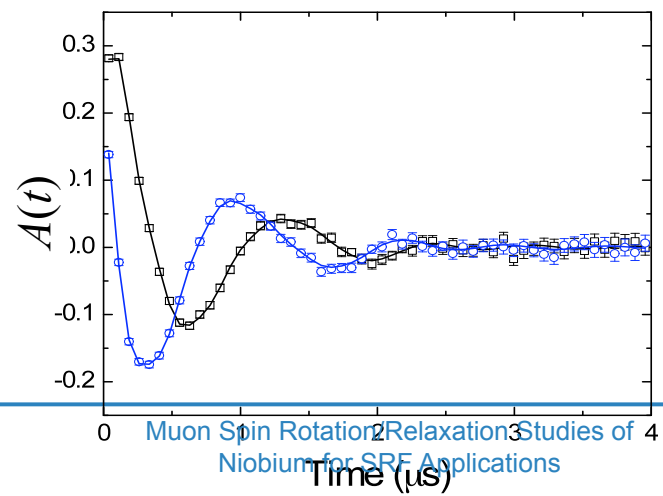
$$G_z(t) = \frac{1}{3} + \frac{2}{3} \left(1 - \Delta^2 t^2\right) \exp\left(-\frac{1}{2} \Delta^2 t^2\right)$$



Magnetic field distribution of a vortex lattice

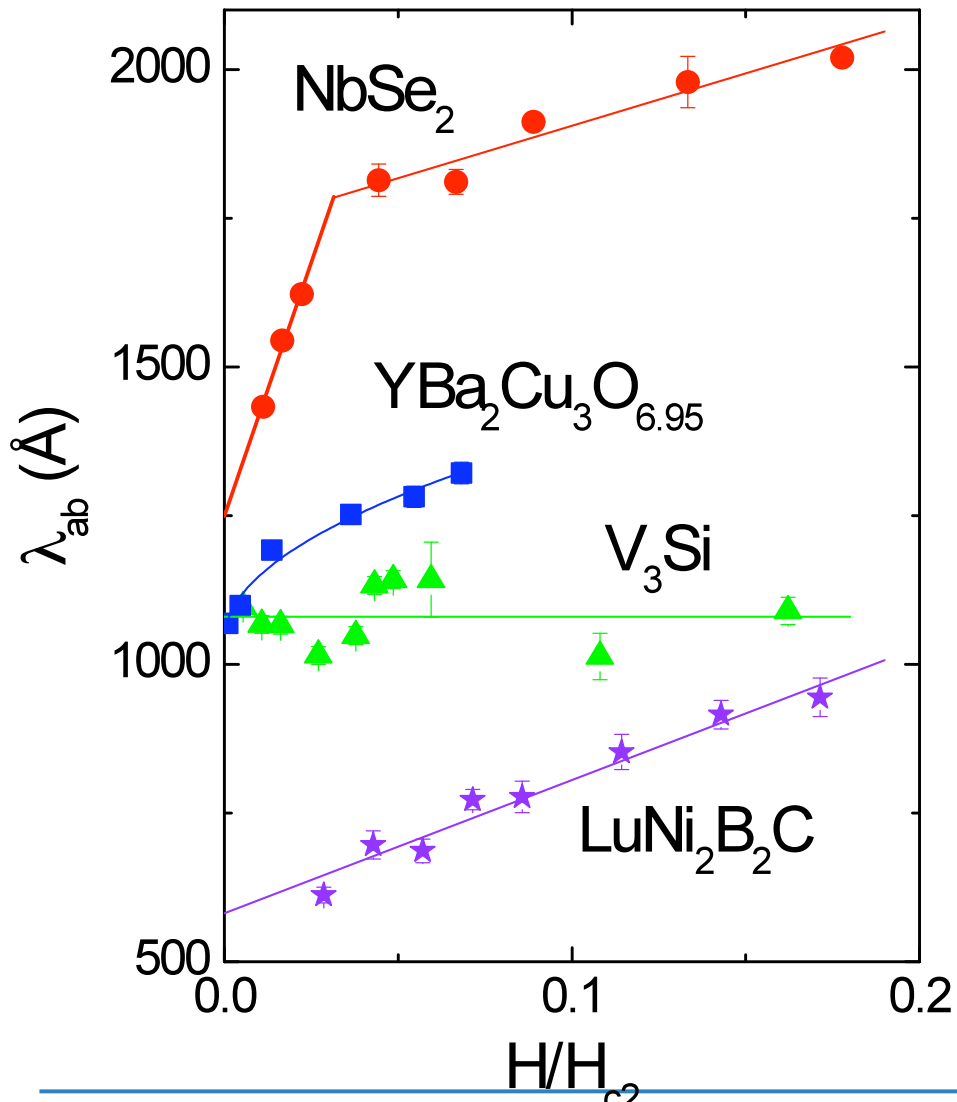


Asymmetry spectrum plotted in a rotating reference frame

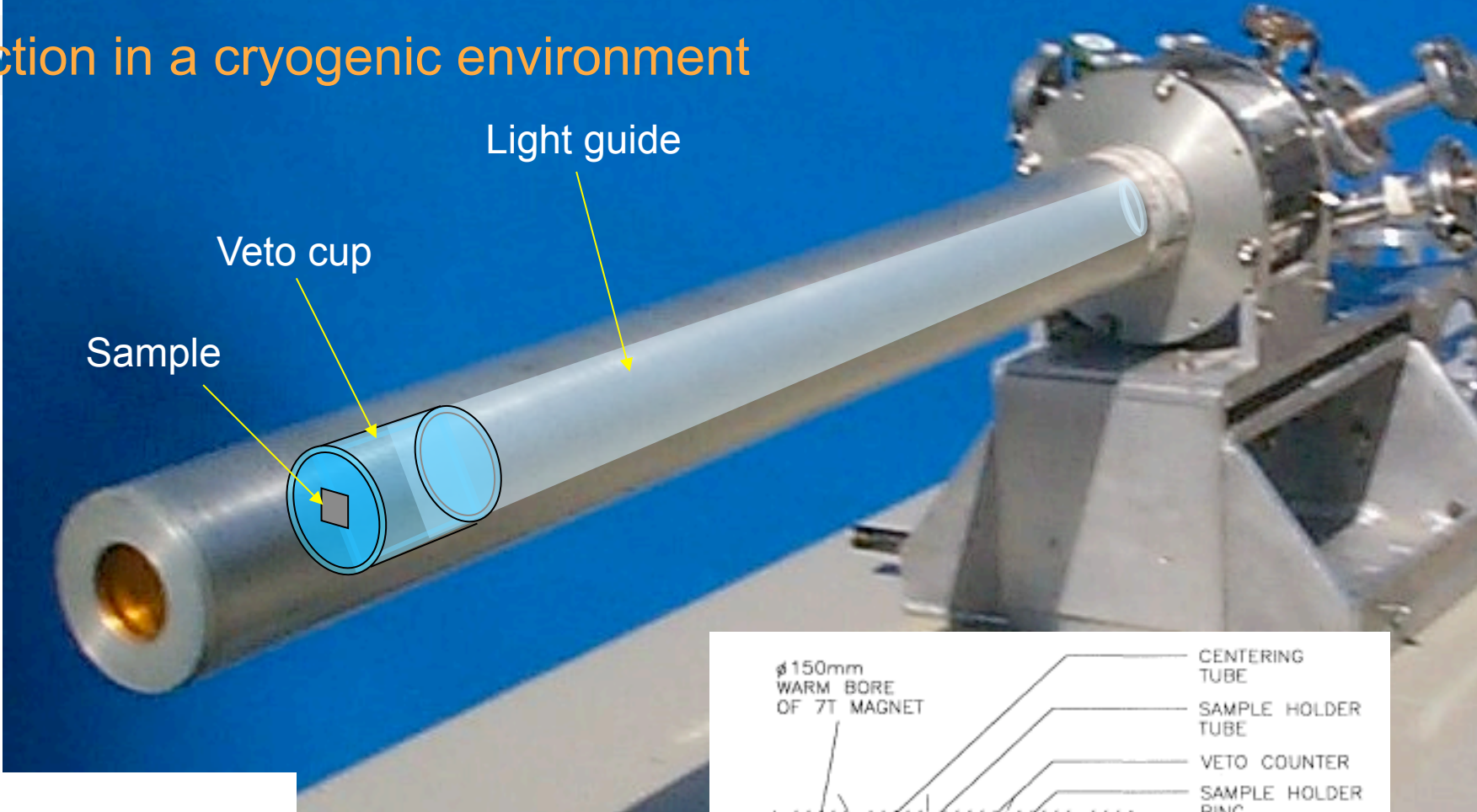


Fourier transform

“Effective” Magnetic Penetration Depth: Magnetic Field Dependence



- V₃Si fully gapped
- LuNi₂B₂C anisotropic gap
- YBa₂Cu₃O_{6.95} $d_{x^2-y^2}$ -wave gap
- NbSe₂ multiband



Muon Spin Rotation/Relaxation Studies of
Niobium for SRF Applications

